Naval Research Laboratory

Washington, DC 20375-5000

NRL Memorandum Report 6523

Electron Beam Propagation Through a Magnetic Wiggler with Random Field Errors

E. ESAREY, W. MARABLE* AND C.M. TANG

Plasma Theory Branch
Plasma Physics Division

**University of Maryland*
College, MD 20742

August 21, 1989

Approved for public release; distribution unlimited.

SECURITY CLASSIFICATION OF THIS PAGE

REPORT DOCUMENTATION PAGE

Form Approved OMB No 0704-0188

1a REPORT SECURITY CLASSIFICATION UNCLASSIFIED	1b RESTRICTIVE MARKINGS
2a. SECURITY CLASSIFICATION AUTHORITY	3 DISTRIBUTION/AVAILABILITY OF REPORT Approved for public release; distribution unlimited.
2b. DECLASSIFICATION/DOWNGRADING SCHEDULE	
4. PERFORMING ORGANIZATION REPORT NUMBER(S) NRL Memorandum Report 6523	5 MONITORING ORGANIZATION REPORT NUMBER(S)
6a. NAME OF PERFORMING ORGANIZATION Naval Research Laboratory; 6b OFFICE SYMBOL (If applicable) Code 4790	7a. NAME OF MONITORING ORGANIZATION
6c. ADDRESS (City, State, and ZIP Code) Washington, DC 20375-5000	7b ADDRESS (City, State, and ZIP Code)
8a. NAME OF FUNDING/SPONSORING ORGANIZATION ONR and DOE; 8b. OFFICE SYMBOL (If applicable)	9 PROCUREMENT INSTRUMENT IDENTIFICATION NUMBER
8c. ADDRESS (City, State, and ZIP Code) ONR Arlington, VA 22217 DOE Washington, DC 20545	10 SOURCE OF FUNDING NUMBERS PROGRAM ELEMENT NO; PROJECT NO; TASK NO; WORK UNIT ACCESSION NO (See page i)

11 TITLE (Include Security Classification)
Electron Beam Propagation through a Magnetic Wiggler with Random Field Errors

12 PERSONAL AUTHOR(S)
Esarey, E., Marable,* W. and Tang, C.M.

13a TYPE OF REPORT	13b TIME COVERED	14 DATE OF REPORT (Year, Month, Day)	15 PAGE COUNT
Interim	FROM ________ TO ______	1989 August 21	61

16 SUPPLEMENTARY NOTATION
*University of Maryland, College Park, MD 20742

17 COSATI CODES			18 SUBJECT TERMS (Continue on reverse if necessary and identify by block number)
FIELD	GROUP	SUB-GROUP	Beam propagation Free electron laser Random errors

19 ABSTRACT (Continue on reverse if necessary and identify by block number)

The effects of random field errors on the propagation of a relativistic electron beam through a wiggler magnet is analyzed both theoretically and numerically. It is found that random field errors give rise to detrimental effects such as a random walk in the transverse position of the beam centroid as well as fluctuations in the parallel energy of the electron beam. This random beam motion is analyzed both for a single realization of a wiggler magnet (a particular arrangement of field errors) and for an ensemble of wiggler magnets with identical statistical properties. Both helical and planar wiggler configurations are studied, with and without the effects of transverse focusing forces. Theoretical expressions

(Continues)

20 DISTRIBUTION/AVAILABILITY OF ABSTRACT ☒ UNCLASSIFIED/UNLIMITED ☐ SAME AS RPT ☐ DTIC USERS	21 ABSTRACT SECURITY CLASSIFICATION UNCLASSIFIED
22a NAME OF RESPONSIBLE INDIVIDUAL E. Esarey	22b TELEPHONE (Include Area Code) (202) 767-2874; 22c OFFICE SYMBOL Code 4790

DD Form 1473, JUN 86 Previous editions are obsolete. SECURITY CLASSIFICATION OF THIS PAGE

S/N 0102-LF-014-6603

SECURITY CLASSIFICATION OF THIS PAGE

10. SOURCE OF FUNDING NUMBERS

PROJECT NO.
ONR Order # 9M0214
DOE # AI05-83ER40117

19. ABSTRACTS (Continued)

are derived for the random electron motion and these results are then confirmed through 3-D particle simulations of electron beam transport including the effects of finite emittance. ~~In the absence of~~ transverse focusing, the rms transverse centroid displacement scales as $z^{3/2}$ and the variance of the parallel energy deviation scales as $z^{1/2}$, ~~where~~ z ~~is~~ the axial propagation distance. Transverse focusing inhibits the random walk of the centroid so that its rms value scales as $z^{1/2}$, but the variance of the parallel energy is only reduced by a factor of $\sqrt{2}$. In a free electron laser (FEL) it may be possible for the random walk of the electrons to become large enough so that the centroids of the radiation and electron beams no longer overlap, thus destroying the FEL interaction and reducing the FEL gain. Likewise, the parallel electron energy deviation may become large enough so that the FEL resonance is no longer maintained, again resulting in a loss in FEL gain.

DD Form 1473, JUN 86 (Reverse)

SECURITY CLASSIFICATION OF THIS PAGE

CONTENTS

ELECTRON BEAM PROPAGATION THROUGH A MAGNETIC WIGGLER WITH RANDOM FIELD ERRORS

I. Introduction

Electron beam propagation through magnetic wigglers has become a topic of recent concern primarily due to its relevance to free electron lasers (FELs). Interest in FELs has become widespread[1] since the FEL offers both a tunable source of radiation from the microwave to the subvisible range as well as the capability for producing intense power levels. The quest for FELs to serve as high power single pass amplifiers has led to the design of long wigglers extending for hundreds of wiggler wavelengths. The design and analysis of such FELs typically assumes the wiggler field to be adequately described by its ideal sinusoidal form. However, the intrinsic imprecisions which occur in the fabrication and assembly of wiggler magnets result in a magnetic field which deviates from the ideal sinusoidal form by some small error, δB. Typical state–of–the–art wiggler construction[2] results in intrinsic field errors of $\delta B/B_w \geq 0.1\%$, where B_w is the peak ideal wiggler magnetic field on axis. These intrinsic field errors lead to detrimental effects which generally increase with the axial length of the wiggler.[3-6] Hence, for long wigglers the detrimental effects of field errors become exceedingly important. These effects, if left uncorrected, may destroy the FEL interaction and lead to a loss in radiation gain.

Physically, the detrimental effects of wiggler errors may be understood as follows. As the electron beam propagates through the wiggler in the axial z–direction, the electrons encounter a series of errors in the transverse magnetic field $\delta \mathbf{B}_\perp$, which are assumed to be random. The beam electrons then experience a series of random transverse $(\mathbf{v}_z \times \delta \mathbf{B}_\perp)$ forces, where $v_z \simeq c$ is the axial velocity of a relativistic electron. This series of random forces results in a random walk of the electron beam centroid, causing the centroid to deviate from the wiggler axis by some amount $\delta x(z)$. Statistically speaking (as will be discussed below), the rms magnitude of transverse beam displacement $\delta x(z)$ generally increases as a function of the axial propagation distance z. In an FEL, the magnitude of the beam displacement $\delta x(z)$ may become large enough to prohibit optical guiding[7] of the radiation which decouples the electron beam *from* the radiation beam (the electron beam centroid no longer overlaps the radiation beam centroid), thus destroying the FEL interaction; or worse yet, the electron beam may deviate sufficiently far off axis so as to hit the wall of the wiggler magnets. Ideally, to avoid such detrimental effects, it may be desirable to keep the magnitude of the beam walk off less than the radius r_b of the electron beam, $|\delta x| < r_b$.

Not only do the wiggler field errors cause the electron beam to walk off axis, the

Manuscript approved June 16, 1989.

errors also cause the parallel energy of the electron beam to deviate from its ideal value (the value in the absence of field errors).[6] As the field errors induce a transverse beam motion (and a transverse energy) through the beam walk off, the errors subsequently alter the parallel energy of the beam, since static magnetic fields do not alter the total beam energy. Statistically, the variance of the deviation in the parallel beam energy $\delta\gamma_{\parallel}(z)$ generally increases as the propagation distance z increases. Here, $\gamma_{\parallel} = (1 - v_z^2/c^2)^{-1/2}$ is the relativistic factor associated with the axial electron motion. In an FEL, the parallel energy deviation $\delta\gamma_{\parallel}(z)$ may increase in magnitude to the point where the wave–particle resonance is no longer maintained, thus destroying the FEL interaction and reducing the overall FEL gain. In order for the electrons to maintain their resonance with the radiation field, it is necessary for the electron parallel energy deviation to be small compared to the intrinsic power efficiency η for FELs in the low or high gain regimes,[8] $|\delta\gamma_{\parallel}/\gamma_{\parallel 0}| < \eta$, where $\gamma_{\parallel 0}$ is the electron parallel energy in the absence of field errors. In the trapped particle regime, the parallel energy deviation must be small compared to the ponderomotive potential created by the FEL radiation:[9] $|\delta\gamma_{\parallel}/\gamma_{\parallel 0}| < |e\phi_p/(\gamma m_0 c^2)|$, where ϕ_p is the ponderomotive potential and m_0 is the electron rest mass.

The effects of random field errors in magnetic undulators were first analyzed by Kincaid.[3] In his work, Kincaid was concerned with how these errors affected the spontaneous radiation spectrum resulting from the passage of an electron beam through the undulator. Kincaid studied the transverse orbit of a single electron in the 1-D limit, neglecting the effects of transverse weak focusing. Kincaid also assumed a specific model for the random errors, in which the axial dependence of the field error associated with a given pole pair was assumed to be a sinusoid extending over half an undulator period (see the discussion in Sec. VI). Elliott and McVey also analyzed the effects of field errors in undulators and wigglers.[4] Again, they were primarily concerned with how these errors affected the spontaneous radiation spectrum (for undulators) or the radiation gain (for wigglers). Elliott and McVey presented theoretical calculations of the transverse orbit of a single electron including the effects of transverse focusing based on a model which assumed that the electrons received discrete independent velocity kicks from field errors at each pole pair. These theoretical calculations were then supported by the results of an FEL simulation code in which the electron dynamic equations were averaged over a wiggler period. Shay and Scharlemann used a similar FEL simulation code to study the effects of field errors on FEL performance.[5] The random walk of the beam including 3-D focusing effects was briefly discussed and plots showing how field errors reduce FEL output power were presented. The works of Kincaid, Elliott and McVey as well as Shay and Scharlemann all

discussed how the detrimental effects of field errors could be reduced by periodic external steering of the electron beam. None of these works, however, directly calculated the effects of random field errors on the parallel energy of the electrons, nor did they perform particle simulations of beam transport in which the electrons are modeled by the full relativistic Lorentz equations (as opposed to a spatial averaged version).

In the following sections, a comprehensive theoretical and numerical analysis is presented determining the effects of random wiggler field errors on relativistic electron beam propagation. Specifically, how random field errors affect the transverse position of the electron beam centroid as well as the parallel electron beam energy will be determined. This study concerns the effects of random, homogeneous errors in the transverse magnetic field $\delta B_{\perp}(z)$ which statistically have zero mean, a finite variance and a finite autocorrelation distance. It is assumed that the field errors $\delta B_{\perp}(z)$ are a function only of the propagation distance z, which is a valid approximation provided that the transverse variations in the field errors are small over the transverse spatial extent of the electron beam. However, 3-D effects are retained in the beam dynamics and in the form for the ideal wiggler field which enables the effects of transverse weak focusing to be studied. In this analysis, it is assumed that there exists an ensemble of wiggler magnets which contain statistically identical magnetic fields. Expressions are derived for an electron beam quantity Q for a particular wiggler realization (a particular member of the ensemble) as well as for the appropriate statistical averages (denoted by angular brackets) over the members of the ensemble, such as the mean $\langle Q \rangle$ and variance squared $\langle Q^2 \rangle - \langle Q \rangle^2$. The theoretical analysis presented below assumes that the relativistic electron beam dynamics may be adequately described by the dynamics of a single electron located at the beam centroid. This assumption is then supported by performing full scale nonlinear 3-D simulations[10] of electron beam propagation including finite emittance and space charge effects.

The remainder of this paper is organized as follows. Section II of this paper presents an analytical treatment of the basic properties of general random field errors. In Sec. III, an analytic theory is developed for electron motion in a helical wiggler with general random errors in the 1-D limit. This theory is generalized to include the 3-D effects of transverse weak focusing in Sec. IV. In Sec. V, analytical results are presented for electron propagation through planar wigglers for the case of flat pole faces as well as for the case of parabolic pole faces. Section VI presents the results of the beam propagation simulation code. This paper then concludes with a summary and discussion of the results in Sec. VII.

II. Random Field Error Statistics

In an actual wiggler magnet, the magnetic field will deviate from the ideal theoretical sinusoidal form, B_w, by some small amount δB. Hence, the total magnetic field will be denoted by

$$\mathbf{B}(x,y,z) = \mathbf{B}_w(x,y,z) + \delta B_x(z)\mathbf{e}_x + \delta B_y(z)\mathbf{e}_y. \tag{1}$$

Throughout the following, the dependence of δB on the transverse coordinates will be neglected. This assumes that $(\delta B(r_{max},z) - \delta B(0,z))^2/\delta B(0,z)^2 \ll 1$, where r_{max} is the maximum transverse displacement of the electron beam from the axis.

In the following analysis, it is assumed that there exists an ensemble of wiggler magnets in which the associated field errors $\delta\mathbf{B}$ exhibit known statistical properties. Specifically, it is assumed that $\langle\delta\mathbf{B}(z)\rangle = 0$ and that the correlation functions for the field errors, $\langle\delta B(z)\delta B(z+\Delta z)\rangle$, are known. Furthermore, it is assumed that the random field errors are homogeneous, that is, the correlation functions $\langle\delta B(z)\delta B(z+\Delta z)\rangle$ are only a function of Δz. These correlation functions are assumed to exhibit the following properties:

$$\begin{aligned}
&\langle\delta B_x(z)\delta B_x(z+\Delta z)\rangle \begin{cases} \equiv \langle\delta B_x^2\rangle, & \text{for } \Delta z = 0 \\ \simeq 0, & \text{for } |\Delta z| > z_{cx}, \end{cases} \\
&\langle\delta B_y(z)\delta B_y(z+\Delta z)\rangle \begin{cases} \equiv \langle\delta B_y^2\rangle, & \text{for } \Delta z = 0 \\ \simeq 0, & \text{for } |\Delta z| > z_{cy}, \end{cases} \\
&\langle\delta B_x(z)\delta B_y(z+\Delta z)\rangle \equiv 0.
\end{aligned} \tag{2}$$

In the above expressions, $\langle\delta B_x^2\rangle$ and $\langle\delta B_y^2\rangle$ are assumed to be constants and represent the mean-squared field errors of the x and y components of the magnetic field. Also, z_{cx} and z_{cy} are the autocorrelation distances for the errors $\delta B_x(z)$ and $\delta B_y(z)$, respectively, which are defined by the expressions

$$\begin{aligned}
&\int_{-\infty}^{\infty} d\Delta z\, \langle\delta B_x(z)\delta B_x(z+\Delta z)\rangle \equiv z_{cx}\langle\delta B_x^2\rangle, \\
&\int_{-\infty}^{\infty} d\Delta z\, \langle\delta B_y(z)\delta B_y(z+\Delta z)\rangle \equiv z_{cy}\langle\delta B_y^2\rangle.
\end{aligned} \tag{3}$$

Physically, z_c is the distance over which the field error $\delta B(z)$ remains coherent (see Fig. 1). Typically, one expects $z_c \simeq \lambda_w/2$, where λ_w is the wavelength of the wiggler field. This implies that the scale length for the field error associated with a given magnet pole is approximately equal to the width of that pole. The last expression in Eq. (2) indicates that the x and y components of the field errors are assumed to be uncorrelated.

Another quantity of interest is the vector potential $\delta A_{x,y}(z)$ associated with the field error $\delta B_{x,y}(z)$. Defining the normalized vector potentials $\delta a = e\delta A/(m_0c^2)$ and $a_w = eB_w/(k_w m_0 c^2)$, where $k_w = 2\pi/\lambda_w$ is the wiggler wavenumber, then

$$\delta a_x = \frac{a_w k_w}{B_w}\int_0^z dz'\delta B_y(z') \quad \text{and} \quad \delta a_y = -\frac{a_w k_w}{B_w}\int_0^z dz'\delta B_x(z'). \tag{4}$$

It then follows that the correlation of the normalized vector potential errors is given by[11,12]

$$\begin{aligned}\langle\delta a_x(z_1)\delta a_x(z_2)\rangle &= \frac{a_w^2 k_w^2}{B_w^2}\int_0^{z_1} dz'\int_0^{z_2} dz''\,\langle\delta B_y(z')\delta B_y(z'')\rangle \\ &\simeq \frac{a_w^2 k_w^2}{B_w^2}\int_0^{z_m} dz'\int_{-\infty}^{\infty} d\Delta z\,\langle\delta B_y(z')\delta B_y(z'+\Delta z)\rangle\left[1+\mathcal{O}\left(\frac{z_{cy}}{z_m}\right)\right] \\ &= 2D_x z_m, \quad D_x \equiv \frac{1}{2}a_w^2\frac{\langle\delta B_y^2\rangle}{B_w^2}k_w^2 z_{cy},\end{aligned} \tag{5}$$

provided $|z_m| > z_{cy}$, where z_m is the smaller of z_1 and z_2. Throughout the following, terms of order $\mathcal{O}(z_c/z)$ will be neglected. Similarly, for the y-component of the normalized vector potential errors, one has

$$\langle\delta a_y(z_1)\delta a_y(z_2)\rangle = 2D_y z_m, \quad D_y \equiv \frac{1}{2}a_w^2\frac{\langle\delta B_x^2\rangle}{B_w^2}k_w^2 z_{cx}, \tag{6}$$

provided $|z_m| > z_{cx}$. The above expressions are used below to calculate the statistical behavior of the random walk and parallel energy deviation of the electrons.

III. Propagation Without Transverse Focusing

As a first step in determining how field errors effect electron beam propagation through a magnetic wiggler, the transverse gradients associated with the wiggler field will be neglected. Such an approximation is valid provided the displacement of the electron beam off axis is much smaller than a wiggler wavelength. This amounts to neglecting the transverse focusing force the electron beam would normally feel as it moves off axis into a region of stronger wiggler strength. In the absence of field errors, this transverse gradient in the wiggler field gives rise to betatron oscillations.[9,13] As is shown in Sec. IV, neglecting the transverse focusing forces is valid provided $(2zk_\beta)^2 << 1$, where $k_\beta = a_w k_w/(\sqrt{2}\gamma)$ is the betatron wavenumber.

The ideal wiggler field is assumed to be helical, and in the 1-D limit, is given by

$$\begin{aligned} \mathbf{B}_w(z) &= B_w\,(\cos k_w z\ \mathbf{e}_x + \sin k_w z\ \mathbf{e}_y)\,, \\ \mathbf{A}_w(z) &= -\frac{B_w}{k_w}\,(\cos k_w z\ \mathbf{e}_x + \sin k_w z\ \mathbf{e}_y)\,, \end{aligned} \tag{7}$$

where $\mathbf{A}_w$ is the vector potential associated with $\mathbf{B}_w$. Generalization of the results below to the case of a planar wiggler is straightforward and is discussed in Sec. V.

Neglecting the transverse gradients, the problem becomes 1-D, and the motion of an electron through the magnetic wiggler is completely described by conservation of perpendicular canonical momentum and conservation of energy,

$$\mathbf{p}_\perp = \frac{e}{c}\mathbf{A}_\perp \quad \text{and} \quad \gamma = \gamma_\parallel \gamma_\perp, \tag{8}$$

where $\mathbf{p}_\perp = \gamma m \mathbf{v}_\perp$ and $\gamma_\perp = (1 + p_\perp^2/m^2c^2)^{1/2}$. Note that γ is a constant of the motion since there is no applied electric field. Writing $\mathbf{v}_\perp = \mathbf{v}_w + \delta\mathbf{v}_\perp$, where $\mathbf{v}_w = c\mathbf{a}_w/\gamma$ is the electron wiggle motion in the ideal wiggler field $\mathbf{B}_w$, then the deviation $\delta\mathbf{v}_\perp$ from this ideal motion is given by $\delta\mathbf{v}_\perp = (c/\gamma)\delta\mathbf{a}_\perp$. Notice that $\langle\delta\mathbf{v}_\perp\rangle = 0$ and that the mean–square perpendicular velocity deviation is given by

$$\langle \delta v_\perp^2 \rangle = \frac{c^2}{\gamma^2} 2D_\perp z, \quad \text{for } |z| > z_{cx,y}, \tag{9}$$

where $D_\perp = D_x + D_y$. Hence, the mean–square perpendicular velocity of the electrons increases linearly with the distance traveled through the wiggler due to the presence of field errors.

A more important quantity, however, is the transverse displacement of the electron orbit off axis. This is obtained from the perpendicular electron velocity by the relation $\mathbf{v}_\perp = v_z d\mathbf{x}_\perp/dz$. Again, writing $\mathbf{x}_\perp = \mathbf{x}_w + \delta\mathbf{x}_\perp$, where $\mathbf{x}_w$ is the electron transverse wiggle orbit in the ideal wiggler field $\mathbf{B}_w$, then the transverse orbit deviation is given by

$$\delta\mathbf{x}_\perp = \frac{1}{\gamma}\int_0^z dz'\delta\mathbf{a}_\perp, \tag{10}$$

where the approximation $v_z = c$ has been made. Again, $\langle\delta\mathbf{x}_\perp\rangle = 0$, and the mean-square transverse displacement is given by

$$\left\langle\delta x_\perp^2\right\rangle = \frac{1}{\gamma^2}\frac{2}{3}D_\perp z^3, \quad \text{for } |z| > z_{cx,y}. \tag{11}$$

The above equation indicates that the rms value of the transverse displacement due to field errors increases as $z^{3/2}$. This expression agrees with the results of Kincaid[3] in which the random walk in 1-D was calculated for a specific field error model (see Sec. VI).

The results for the mean-square values of the electron's perpendicular velocity and orbit given in Eqs. (9) and (11) may be understood through the following physical arguments. The x-component of the equation of motion for the electron in the combined magnetic field is given by

$$\gamma m_0\frac{d}{dt}v_x = eB_w\sin k_w z + e\delta B_y. \tag{12}$$

The first term on the right of the above equation is the force due to the ideal wiggler field whereas the second term is the random force due to the field errors. Hence, the error δB_y produces random velocity kicks δv_x. Such a process is described statistically as "velocity-space diffusion" and one expects the mean-square velocity to scale as $\left\langle\delta v_x^2\right\rangle \sim 2D_x z$, where D_x is the diffusion coefficient. Similarly, $\delta x = \int dt\delta v_x$ and, hence, δx is a "time-integrated diffusion process", which exhibits the generic form $\left\langle\delta x^2\right\rangle \sim (2/3)D_x z^3$. One should keep in mind that the above relations only hold for long "times", that is, for $(z/z_c)^2 >> 1$, where z_c is the autocorrelation distance for the random force δB_y.

Another quantity which is of interest is the parallel energy of the electrons $\gamma_\parallel$. The statistical behavior of $\gamma_\parallel$ is calculated from the relation $\gamma_\parallel = \gamma/\gamma_\perp$, where γ is a constant of the motion and $\gamma_\perp = (1+\gamma^2\beta_\perp^2)^{1/2}$. Here $\beta = \mathrm{v}/c$ is the normalized electron velocity. Using the above results, one can write $\beta_\perp = \beta_{\perp 0} + \delta\beta_\perp$, where $\beta_{\perp 0}$ is the normalized perpendicular velocity in the absence of field errors. Defining $\gamma_{\perp 0} = (1+\gamma^2\beta_{\perp 0}^2)^{1/2}$ and $\gamma_{\parallel 0} = \gamma/\gamma_{\perp 0}$, then the parallel electron energy is given by

$$\gamma_\parallel = \gamma_{\parallel 0}\left[1+\gamma_{\parallel 0}^2\left(2\beta_{\perp 0}\cdot\delta\beta_\perp + \delta\beta_\perp^2\right)\right]^{-1/2}. \tag{13}$$

For the present case of electron propagation in the 1-D limit, $\beta_{\perp 0} = a_w/\gamma$ and $\delta\beta_\perp = \delta a_\perp/\gamma$. The statistical properties of the parallel energy are easily calculated by expanding the expressions for $\gamma_\parallel$ and $\gamma_\parallel^2$ to include all terms of order $\delta a_\perp^2$. Specifically, the mean $\langle\gamma_\parallel\rangle$ and the square of the variance $\langle\gamma_\parallel^2\rangle - \langle\gamma_\parallel\rangle^2$ of the parallel energy are given by the expressions

$$\frac{\langle\gamma_\parallel\rangle - \gamma_{\parallel 0}}{\gamma_{\parallel 0}} = -\frac{z}{\gamma_{\perp 0}^4}\left[\left(1 - \frac{a_w^2}{2}\right)(D_x + D_y) - \frac{3}{2}a_w^2(D_x - D_y)\cos 2k_w z\right], \tag{14a}$$

$$\frac{\langle\gamma_\parallel^2\rangle - \langle\gamma_\parallel\rangle^2}{\gamma_{\parallel 0}^2} = \frac{z a_w^2}{\gamma_{\perp 0}^4}\left[(D_x + D_y) + (D_x - D_y)\cos 2k_w z\right], \tag{14b}$$

where $\gamma_{\perp 0} = (1 + a_w^2)^{1/2}$. In the limit $D_x = D_y$ ($\langle\delta B_x^2\rangle z_{cx} = \langle\delta B_y^2\rangle z_{cy}$), the above expressions reduce to

$$\frac{\langle\gamma_\parallel\rangle - \gamma_{\parallel 0}}{\gamma_{\parallel 0}} = -\frac{(1 - a_w^2/2)}{(1 + a_w^2)^2}\left\langle\frac{\delta B^2}{B_w^2}\right\rangle a_w^2 k_w^2 z_c z, \tag{15a}$$

$$\frac{\langle\gamma_\parallel^2\rangle - \langle\gamma_\parallel\rangle^2}{\gamma_{\parallel 0}^2} = \frac{a_w^2}{(1 + a_w^2)^2}\left\langle\frac{\delta B^2}{B_w^2}\right\rangle a_w^2 k_w^2 z_c z. \tag{15b}$$

As before, the above formulas apply provided $(z/z_c)^2 >> 1$. Notice that $\langle\gamma_\parallel\rangle - \gamma_{\parallel 0}$ may either be positive or negative, depending on whether or not $a_w^2/2 > 1$. This indicates that it is possible for the field errors to perturb the electrons in such a way that the perpendicular energy in the ideal wiggle motion of the electrons is converted into parallel energy. Also, notice that the variance of the parallel energy deviation increases as $\sqrt{z}$.

IV. Propagation with Transverse Focusing

Transverse focusing of an electron beam results from the transverse gradients in the wiggler magnetic fields. Specifically, as an electron beam moves off axis it also moves into a region of higher magnetic field which tends to focus the electron beam back toward the axis. This weak focusing, in the absence of field errors, produces beam oscillations at the betatron[9,13] wavelength $\lambda_\beta = \sqrt{2}\gamma\lambda_w/a_w$. Hence, in the presence of field errors, one expects that as the electron beam begins to random walk off axis, the weak focusing forces tend to steer the beam back towards the axis, thus, diminishing the magnitude of the transverse random walk of the beam centroid.

To study the transverse motion of an electron beam in the presence of weak focusing, a helical wiggler field is assumed with a normalized vector potential given by the following model equations:

$$\begin{aligned} a_x &= a_w\left(1 + k_w^2 y^2/2\right)\cos k_w z + \delta a_x(z), \\ a_y &= a_w\left(1 + k_w^2 x^2/2\right)\cos k_w z + \delta a_y(z), \end{aligned} \tag{16}$$

where it is assumed $k_w^2 x^2 << 1$ and $k_w^2 y^2 << 1$. This model gives an adequate approximation to a realizable helical wiggler field near the axis.[14]

The electron motion is described by the relativistic Lorentz equation, which may be written in the following form:

$$\begin{aligned} \frac{d}{dt}\left(v_x - \frac{c}{\gamma}a_x\right) &= -\frac{c}{\gamma}\mathbf{v}\cdot\frac{\partial}{\partial x}\mathbf{a}, \\ \frac{d}{dt}\left(v_y - \frac{c}{\gamma}a_y\right) &= -\frac{c}{\gamma}\mathbf{v}\cdot\frac{\partial}{\partial y}\mathbf{a}. \end{aligned} \tag{17}$$

The above transverse equations of motion will be solved in a parameter regime assuming the following approximations. Physically, one expects the perpendicular electron motion to be dominated by a fast wiggle motion $v_{\perp f}$ and a slower random motion $\delta v_\perp$ resulting from the finite field errors. Hence, it will be assumed $\delta v_\perp^2/v_{\perp f}^2 << 1$. Also, cases of physical interest occur when the transverse random walk $\delta x_\perp$ of the electrons becomes much greater than the amplitude of the fast wiggle motion $x_{\perp f}$. Hence, it will be assumed that $x_{\perp f}^2/\delta x_\perp^2 << 1$. As will be shown below, these two inequalities imply that

$$\frac{\lambda_w^2}{\lambda_\beta^2} << \left\langle\frac{\delta B^2}{B_w^2}\right\rangle 2\pi^2\frac{z}{\lambda_w} << 1. \tag{18}$$

In actuality, the results derived below describing the random motion of the electrons are somewhat more general than the above inequalities imply. However, such a derivation becomes too detailed to be presented in this text. Instead, the above inequalities will be assumed, which corresponds to the region of physical interest, which greatly simplifies the derivation.

The x–component of the electron motion is calculated by letting $v_x = v_{xf} + \delta v_x$, where $v_{xf} = (ca_w/\gamma)(1 + k_w^2 y^2/2)\cos k_w z$ is the fast wiggle oscillation in the local wiggler field. Assuming $\delta v_x^2/v_f^2 << 1$ and $x_f^2/\delta x^2 << 1$, where $d\delta x/dt = \delta v_x$ and $dx_f/dt = v_{xf}$, gives

$$\frac{d^2}{dz^2}\delta x + k_\beta^2 \delta x\,(1 - \cos 2k_w z) = \frac{1}{\gamma}\frac{d}{dz}\delta a_x, \tag{19}$$

where $k_\beta = a_w k_w/(\sqrt{2}\gamma)$ is the betatron wavenumber. In deriving the above equation, a change of variables from the independent variable t to the independent variable z was made along with $d/dt = v_z d/dz \simeq cd/dz$. Letting $\delta x = \delta x_s + \delta x_f$ and assuming $\delta x_f^2/\delta x_s^2 << 1$, gives $\delta x_f \simeq -(k_\beta/2k_w)^2 \delta x_s \cos 2k_w z$ and

$$\frac{d^2}{dz^2}\delta x_s + k_\beta^2 \delta x_s = \frac{a_w}{\gamma} k_w \frac{\delta B_y}{B_w}. \tag{20a}$$

Clearly, δx_f represents a small correction to δx on the fast time scale $d/dz \sim 2k_w$ which shall be neglected. In the above equation for δx_s, the second term on the left represents the weak focusing force from the transverse gradient of the wiggler field and the term on the right represents the random force from the finite field error.

Similarly, the y–component of the motion can be calculated by letting $v_y = v_{yf} + \delta v_y$, where $v_{yf} = (ca_w/\gamma)(1 + k_w^2 x^2/2)\sin k_w z$, and assuming $\delta v_y^2/v_{yf}^2 << 1$ and $y_f^2/\delta y^2 << 1$. Setting $\delta y = \delta y_s + \delta y_f$ gives $\delta y_f = (k_\beta/2k_w)^2 \delta y_s \cos 2k_w z$ and

$$\frac{d^2}{dz^2}\delta y_s + k_\beta^2 \delta y_s = -\frac{a_w}{\gamma} k_w \frac{\delta B_x}{B_w}. \tag{20b}$$

Solving for the random orbits δx_s and δy_s is straightforward and one finds

$$\begin{aligned}\delta x_s(z) &= -\frac{a_w k_w}{\gamma k_\beta}\int_0^z dz' \sin k_\beta\,(z' - z)\,\frac{\delta B_y(z')}{B_w},\\ \delta y_s(z) &= \frac{a_w k_w}{\gamma k_\beta}\int_0^z dz' \sin k_\beta\,(z' - z)\,\frac{\delta B_x(z')}{B_w}.\end{aligned} \tag{21}$$

Likewise, the random perpendicular velocities $\delta\beta_{xs} = \delta v_{xs}/c$ and $\delta\beta_{ys} = \delta v_{ys}/c$ are given by

$$\begin{aligned}\delta\beta_{xs}(z) &= \frac{a_w k_w}{\gamma}\int_0^z dz' \cos k_\beta\,(z' - z)\,\frac{\delta B_y(z')}{B_w},\\ \delta\beta_{ys}(z) &= -\frac{a_w k_w}{\gamma}\int_0^z dz' \cos k_\beta\,(z' - z)\,\frac{\delta B_x(z')}{B_w}.\end{aligned} \tag{22}$$

Physically, δx_s and δy_s represent diffusing betatron orbits which are the result of random velocity kicks from the finite field errors in the presence of weak focusing forces.

In order to calculate the mean-square values for the transverse electron orbits, it is necessary to evaluate the following expression:

$$
\begin{aligned}
&\int_0^z dz' \int_0^z dz'' \sin k_\beta (z' - z) \sin k_\beta (z'' - z) \langle \delta B(z') \delta B(z'') \rangle \\
&\quad \simeq \int_0^z dz' \int_{-\infty}^{\infty} d\Delta z \frac{1}{2} \left[\cos k_\beta \Delta z - \cos k_\beta (2z' - 2z + \Delta z) \right] \\
&\qquad\qquad \times \langle \delta B(z') \delta B(z' + \Delta z) \rangle \left[1 + \mathcal{O}\left(\frac{z_c}{z} \right) \right] \qquad (23a) \\
&\quad \simeq \int_0^z dz' \frac{1}{2} \left[1 - \cos 2k_\beta (z' - z) \right] \langle \delta B^2 \rangle z_c \left[1 + \mathcal{O}\left(\frac{z_c}{z} \right) + \mathcal{O}(k_\beta z_c) \right] \\
&\quad = \frac{1}{2} \left(z - \frac{\sin 2k_\beta z}{2k_\beta} \right) \langle \delta B^2 \rangle z_c \left[1 + \mathcal{O}\left(\frac{z_c}{z} \right) + \mathcal{O}(k_\beta z_c) \right],
\end{aligned}
$$

where $(z_c/z)^2 << 1$ and $(k_\beta z_c)^2 << 1$ has been assumed. In evaluating the above expressions, it has been assumed that the correlation function $\langle \delta B(z) \delta B(z + \Delta z) \rangle$ is independent of z and becomes zero for $|\Delta z| > z_c$, as is discussed in Sec. II. Similarly, one can show

$$
\begin{aligned}
&\int_0^z dz' \int_0^z dz'' \cos k_\beta (z' - z) \cos k_\beta (z'' - z) \langle \delta B(z') \delta B(z'') \rangle \\
&\quad \simeq \frac{1}{2} \left(z + \frac{\sin 2k_\beta z}{2k_\beta} \right) \langle \delta B^2 \rangle z_c \left[1 + \mathcal{O}\left(\frac{z_c}{z} \right) + \mathcal{O}(k_\beta z_c) \right]. \qquad (23b)
\end{aligned}
$$

These expressions are then used to calculate the statistical averages of the transverse orbits and, in doing so, terms of order $\mathcal{O}(z_c/z)$ and $\mathcal{O}(k_\beta z_c)$ will be neglected.

Statistically averaging over the wiggler ensemble gives the following expressions for the mean-square quantities:

$$
\langle \delta x_s^2 \rangle = \left(\frac{a_w k_w}{\gamma k_\beta} \right)^2 \left\langle \frac{\delta B_y^2}{B_w^2} \right\rangle \frac{z_{cy}}{2} \left(z - \frac{\sin 2k_\beta z}{2k_\beta} \right), \qquad (24a)
$$

$$
\langle \delta y_s^2 \rangle = \left(\frac{a_w k_w}{\gamma k_\beta} \right)^2 \left\langle \frac{\delta B_x^2}{B_w^2} \right\rangle \frac{z_{cx}}{2} \left(z - \frac{\sin 2k_\beta z}{2k_\beta} \right), \qquad (24b)
$$

$$
\langle \delta \beta_{xs}^2 \rangle = \left(\frac{a_w k_w}{\gamma} \right)^2 \left\langle \frac{\delta B_y^2}{B_w^2} \right\rangle \frac{z_{cy}}{2} \left(z + \frac{\sin 2k_\beta z}{2k_\beta} \right), \qquad (25a)
$$

$$
\langle \delta \beta_{ys}^2 \rangle = \left(\frac{a_w k_w}{\gamma} \right)^2 \left\langle \frac{\delta B_x^2}{B_w^2} \right\rangle \frac{z_{cx}}{2} \left(z + \frac{\sin 2k_\beta z}{2k_\beta} \right). \qquad (25b)
$$

Notice that the above expressions reduce to the corresponding 1-D expressions in the limit $(2k_\beta z)^2 << 1$. The above expressions indicate that, in the large z limit, $\langle \delta x_s^2 \rangle^{1/2} \sim \langle \delta y_s^2 \rangle^{1/2} \sim z^{1/2}$ (as opposed to $z^{3/2}$ in the 1-D limit). This argees with the results of Elliott and McVey[4] and of Shay and Scharlemann.[5] Hence, weak focusing significantly reduces the magnitude of the transverse spatial random walk of the beam centroid. Furthermore, notice that $\langle \delta x_s^2 \rangle^{1/2} \sim \langle \delta y_s^2 \rangle^{1/2} \sim 1/k_\beta$ and, hence, additional external focusing (which increases the effective value of k_β) subsequently reduces the transverse displacement of the beam centroid. Notice, however, that $\langle \delta \beta_{xs}^2 \rangle^{1/2} \sim \langle \delta \beta_{ys}^2 \rangle^{1/2} \sim z^{1/2}$, as is the case in the 1-D limit. Hence, in the large z limit, weak focusing only reduces the value of $\langle \delta \beta_{xs}^2 \rangle^{1/2}$ and $\langle \delta \beta_{ys}^2 \rangle^{1/2}$ by a factor of root two as compared to the 1-D values.

It is also of interest to determine how the finite field errors affect the parallel energy of the electrons in the presence of weak focusing. An expression for the parallel energy $\gamma_\parallel$ is easily obtained through conservation of energy $\gamma_\parallel = \gamma/\gamma_\perp$ provided the perpendicular motion is known, $\gamma_\perp^2 = 1 + \gamma^2\beta_\perp^2$. Using the above results, one has $\beta_\perp = \beta_{\perp f} + \delta\beta_{\perp s}$, where $\beta_{\perp f}$ is the fast wiggle oscillation in the local wiggler field and $\delta\beta_{\perp s}$ is the random component of the orbit due to finite field errors. It is then straightforward to calculate the various statistical moments of $\gamma_\parallel$, such as the mean $\langle\gamma_\parallel\rangle$ and the square of the variance $\langle\gamma_\parallel^2\rangle - \langle\gamma_\parallel\rangle^2$. This is done by expanding the corresponding expressions for $\gamma_\parallel$ and $\gamma_\parallel^2$ to second order in $\delta B/B_w$. One finds

$$\frac{\langle\gamma_\parallel\rangle - \gamma_{\parallel 0}}{\gamma_{\parallel 0}} = \frac{1}{\gamma_{\perp 0}^4}\left\{(D_x + D_y)\left[-\left(1+\frac{a_w^2}{4}\right)z + \frac{3a_w^2}{4}\frac{\sin 2k_\beta z}{2k_\beta}\right]\right.$$
$$\left. + (D_x - D_y)\left[\left(\frac{1}{2}+\frac{5a_w^2}{4}\right)z - \left(\frac{1}{2}-\frac{a_{w0}^2}{4}\right)\frac{\sin 2k_\beta z}{2k_\beta}\right]\cos 2k_w z\right\}, \quad (26a)$$

$$\frac{\langle\gamma_\parallel^2\rangle - \langle\gamma_\parallel\rangle^2}{\gamma_{\parallel 0}^2} = \frac{a_w^2}{2\gamma_{\perp 0}^4}\left[(D_x + D_y) + (D_x - D_y)\cos 2k_w z\right]\left(z + \frac{\sin 2k_\beta z}{2k_\beta}\right). \quad (26b)$$

For the case $D_x = D_y$, the above equations reduce to

$$\frac{\langle\gamma_\parallel\rangle - \gamma_{\parallel 0}}{\gamma_{\parallel 0}} = \left(\frac{a_w k_w}{1+a_w^2}\right)^2 \left\langle\frac{\delta B^2}{B_w^2}\right\rangle z_c\left[-\left(1+\frac{a_w^2}{4}\right)z + \frac{3a_w^2}{4}\frac{\sin 2k_\beta z}{2k_\beta}\right], \quad (27a)$$

$$\frac{\langle\gamma_\parallel^2\rangle - \langle\gamma_\parallel\rangle^2}{\gamma_{\parallel 0}^2} = \left(\frac{a_w k_w}{1+a_w^2}\right)^2 \left\langle\frac{\delta B^2}{B_w^2}\right\rangle \frac{a_w^2 z_c}{2}\left(z + \frac{\sin 2k_\beta z}{2k_\beta}\right). \quad (27b)$$

Notice that the above expressions reduce to the 1-D expressions in the limit $(2k_\beta z)^2 << 1$. Furthermore, in the large z limit, both $\langle\gamma_\parallel\rangle \sim z$ and $\langle\gamma_\parallel^2\rangle - \langle\gamma_\parallel\rangle^2 \sim z$, as was the case in the 1-D limit. For the 3-D expressions in the large z limit, however, $\langle\gamma_\parallel\rangle - \gamma_{\parallel 0} < 0$ and $\langle\gamma_\parallel^2\rangle - \langle\gamma_\parallel\rangle^2$ has been reduced by a factor of two as compared to the 1-D value.

V. Propagation Through Planar Wigglers

The results presented above are for wigglers with helical fields. It is straightforward to generalize these results to planar wigglers with linearly polarized fields. The electron motion is analyzed using the methods presented in the previous sections, hence, the details of such calculations will not be repeated. Below, results are presented for planar wigglers of two types: *i*) planar wigglers with flat pole faces and *ii*) planar wigglers with parabolic pole faces.

i) Flat pole faces. Consider a planar wiggler with flat pole faces with a magnetic field described by the normalized vector potential

$$\mathbf{a} = a_w \cosh k_w y \cos k_w z \mathbf{e}_x + \delta a_x(z)\mathbf{e}_x + \delta a_y(z)\mathbf{e}_y. \tag{28}$$

The above vector potential gives a magnetic field primarily in the y–direction which exhibits transverse gradients also in the y–direction. Hence, intuition indicates that the electrons will experience wiggle oscillations in the x–direction and weak focusing in the y–direction.

The x–component of the electron motion consists of fast wiggle oscillations in the local wiggler field plus random velocity kicks in the absence of weak focusing: $\beta_x = \beta_{xf} + \delta\beta_x$, where $\beta_{xf} = (a_w/\gamma)(1 + k_w^2 y^2/2)\cos k_w z$ and $\delta\beta = \delta a_x/\gamma$. Hence, the random part of the orbit δx is described by

$$\delta x(z) = \frac{a_w k_w}{\gamma}\int_0^z dz' \int_0^{z'} dz'' \frac{\delta B_y(z'')}{B_w} \text{ and } \langle \delta x^2 \rangle = \left(\frac{a_w k_w}{\gamma}\right)^2 \left\langle \frac{\delta B_y^2}{B_w^2} \right\rangle z_{cy} \frac{z^3}{3}. \tag{29}$$

The y–component of the electron motion consists of a random orbit δy including the effects of weak focusing. One finds $\delta y = \delta y_s + \delta y_f$, where $\delta y_f = (k_\beta^2/4k_w^2)\delta y_s \cos 2k_w z$ is a small correction to δy which shall be neglected. The random orbit δy_s is described by

$$\begin{aligned} \delta y_s(z) &= \frac{a_w k_w}{\gamma k_\beta}\int_0^z dz' \sin k_\beta (z'-z)\, \frac{\delta B_x(z')}{B_w}, \\ \langle \delta y_s^2 \rangle &= \left(\frac{a_w k_w}{\gamma k_\beta}\right)^2 \left\langle \frac{\delta B_x^2}{B_w^2} \right\rangle \frac{z_{cx}}{2}\left(z - \frac{\sin 2k_\beta z}{2k_\beta}\right). \end{aligned} \tag{30}$$

It is also straightforward to calculate how the field errors affect the parallel energy of the electrons. One finds, to second order in $|\delta B/B_w|$, that the mean and the square of the variance of $\gamma_\parallel$ are given by

$$\frac{\langle\gamma_\parallel\rangle - \gamma_{\parallel 0}}{\gamma_{\parallel 0}} = -\left(\frac{a_w k_w}{\gamma_{\perp 0}}\right)^2 \left\{\frac{1}{2}\left\langle\frac{\delta B_x^2}{B_w^2}\right\rangle z_{cx}\left[z + \frac{1}{2}\cos 2k_w z\left(z - \frac{\sin 2k_\beta z}{2k_\beta}\right)\right]\right.$$

$$\left. - \left\langle\frac{\delta B_y^2}{B_w^2}\right\rangle z_{cy} z\left(1 - \frac{3}{2\gamma_{\perp 0}^2}\right)\right\}, \quad (31a)$$

$$\frac{\langle\gamma_\parallel^2\rangle - \langle\gamma_\parallel\rangle^2}{\gamma_{\parallel 0}^2} = \left(\frac{a_w k_w}{\gamma_{\perp 0}}\right)^2 \left\langle\frac{\delta B_y^2}{B_w^2}\right\rangle z_{cy} z\left(1 - \frac{1}{\gamma_{\perp 0}^2}\right), \quad (31b)$$

where $\gamma_{\perp 0} = (1+a_w^2\cos^2 k_w z)^{1/2}$. Notice that the above expressions have not been averaged over a wiggler period.

Hence, for flat pole faces, in the x–direction in which there are no focusing forces, the rms value for the orbit displacement scales as $z^{3/2}$. In the y–direction, the focusing forces inhibit the orbit walk off which then scales as $z^{1/2}$ in the large z limit. Notice that both the mean and the square of the variance of the parallel energy scale as z, as was true for the case of a helical wiggler, with or without transverse focusing.

ii) Parabolic pole faces. Consider a planar wiggler with parabolic pole faces where the normalized vector potential is given by

$$\begin{aligned} a_x &= a_w \cosh\left(k_w x/\sqrt{2}\right)\cosh\left(k_w y/\sqrt{2}\right)\cos k_w z + \delta a_x(z), \\ a_y &= -a_w \sinh\left(k_w x/\sqrt{2}\right)\sinh\left(k_w y/\sqrt{2}\right)\cos k_w z + \delta a_y(z). \end{aligned} \quad (32)$$

Notice that this is for the special case of equal focusing in the x– and y–directions; that is, $k_x^2 = k_y^2$ where $k_x^2 + k_y^2 = k_w^2$. The above vector potential gives a magnetic field primarily in the y–direction which exhibits transverse gradients in both the x– and y–directions. This indicates that the electrons will experience wiggle oscillations in the x–direction and the random transverse orbits will be modified to include weak focusing in both the x– and y–directions.

The x–component of the electron motion consists of fast wiggle oscillations in the local wiggler field plus random velocity kicks in the presence of weak focusing: $\beta_x = \beta_{xf} + \delta\beta_x$, where $\beta_{xf} \simeq (a_w/\gamma)(1 + k_w^2 x^2/4 + k_w^2 y^2/4)\cos k_w z$. The random conponent of the orbit δx can be written as $\delta x = \delta x_s + \delta x_f$, where δx_f is a small correction to the random orbit $\delta x_f \simeq (k_\beta^2/8k_w^2)\delta x_s \cos 2k_w z$, and where δx_s is described by

$$\delta x_s(z) = -\sqrt{2}\frac{a_w k_w}{\gamma k_\beta}\int_0^z dz' \sin\frac{k_\beta}{\sqrt{2}}(z'-z)\frac{\delta B_y(z')}{B_w},$$
$$\langle \delta x_s^2\rangle = \left(\frac{a_w k_w}{\gamma k_\beta}\right)^2 \left\langle\frac{\delta B_y^2}{B_w^2}\right\rangle z_{cy}\left(z - \frac{\sin\sqrt{2}k_\beta z}{\sqrt{2}k_\beta}\right). \quad (33)$$

Similarly, the y–component of the motion is described by $\beta_y = \beta_{yf} + \delta\beta_y$, where $\beta_{yf} \simeq -(a_w/2\gamma)k_w^2 xy\cos k_w z$. The random component of the orbit δy can be written as $\delta y = \delta y_s + \delta y_f$, where δy_f is a small correction to the random orbit $\delta y_f \simeq (k_\beta^2/8k_w^2)\delta y_s \cos 2k_w z$, and where δy_s is described by

$$\delta y_s(z) = \sqrt{2}\frac{a_w k_w}{\gamma k_\beta}\int_0^z dz' \sin\frac{k_\beta}{\sqrt{2}}(z'-z)\frac{\delta B_x(z')}{B_w},$$
$$\langle \delta y_s^2\rangle = \left(\frac{a_w k_w}{\gamma k_\beta}\right)^2 \left\langle\frac{\delta B_x^2}{B_w^2}\right\rangle z_{cx}\left(z - \frac{\sin\sqrt{2}k_\beta z}{\sqrt{2}k_\beta}\right). \quad (34)$$

Notice that the above expressions for the random orbits δx_s and δy_s are identical to those expressions for a helical wiggler with transverse focusing except that k_β now must be replaced by $k_\beta/\sqrt{2}$.

It is also straightforward to calculate how the field errors effect the parallel energy of the electrons in a planar wiggler with parabolic pole faces. One finds, to second order in $|\delta B/B_w|$, that the mean and the square of the variance of $\gamma_\parallel$ are given by

$$\frac{\langle\gamma_\parallel\rangle - \gamma_{\parallel 0}}{\gamma_{\parallel 0}} = -\left(\frac{a_w k_w}{\sqrt{2}\gamma_{\perp 0}}\right)^2 \left\{\left(\left\langle\frac{\delta B_x^2}{B_w^2}\right\rangle z_{cx} + \left\langle\frac{\delta B_y^2}{B_w^2}\right\rangle z_{cy}\right)\left[z + \frac{1}{2}\cos 2k_w z\left(z - \frac{\sin\sqrt{2}k_\beta z}{\sqrt{2}k_\beta}\right)\right] - \left\langle\frac{\delta B_y^2}{B_w^2}\right\rangle\frac{3z_{cy}}{2}\left(1 - \frac{1}{\gamma_{\perp 0}^2}\right)\left(z + \frac{\sin\sqrt{2}k_\beta z}{\sqrt{2}k_\beta}\right)\right\}, \quad (35a)$$

$$\frac{\langle\gamma_\parallel^2\rangle - \langle\gamma_\parallel\rangle^2}{\gamma_{\parallel 0}^2} = \left(\frac{a_w k_w}{\gamma_{\perp 0}}\right)^2 \left\langle\frac{\delta B_y^2}{B_w^2}\right\rangle\frac{z_{cy}}{2}\left(1 - \frac{1}{\gamma_{\perp 0}^2}\right)\left(z + \frac{\sin\sqrt{2}k_\beta z}{\sqrt{2}k_\beta}\right), \quad (35b)$$

where $\gamma_{\perp 0} = (1 + a_w^2\cos^2 k_w z)^{1/2}$.

Hence, for parabolic pole faces, transverse weak focusing exists in both the x– and y–directions and the rms value of the orbit displacement in both transverse directions scales as $z^{1/2}$ (in the large z limit). Notice that the mean and square of the variance of the parallel energy scale as z, as is the case for all the wigglers examined.

VI. Numerical Simulations

In order to verify the above analytical theory and results, a numerical code was developed[10] to perform full scale simulations of electron beam transport through magnetic wigglers. This code is a fully 3-D particle simulation which includes finite beam emittance and space charge effects. This code simulates beam transport in either helical or planar wiggler configurations, with or without transverse weak focusing, and has the capabilities of including finite wiggler field errors. Once the magnetic field configuration is specified, electron motion is simulated by solving the relativistic Lorentz force equation.

As an example, electron beam transport was studied in a helical wiggler with finite field errors. The magnetic field was modeled by the following expressions:

$$B_x = B_w \left[\left(1 + \frac{k_w^2 r^2}{8}\right) \cos k_w z + \frac{k_w^2}{4} \left(x^2 \cos k_w z + xy \sin k_w z\right) \right] + \delta B_x(z), \quad (36a)$$

$$B_y = B_w \left[\left(1 + \frac{k_w^2 r^2}{8}\right) \sin k_w z + \frac{k_w^2}{4} \left(xy \cos k_w z + y^2 \sin k_w z\right) \right] + \delta B_y(z), \quad (36b)$$

$$B_z = B_w k_w \left(1 + \frac{k_w^2 r^2}{8}\right) \left(y \cos k_w z - x \sin k_w z\right), \quad (36c)$$

where it has been assumed $k_w^2 r^2 \equiv k_w^2 (x^2 + y^2) << 1$.

The functional form of the field errors $\delta B(z)$ was chosen as follows. It is assumed that the field error $\delta B_n(z_n)$ at the center ($z = z_n$) of the n^{th} pair of magnet poles is a random quantity uncorrelated with the field error $\delta B_m(z_m)$ associated with the center of the m^{th} pair of poles, where $m \neq n$. Furthermore, in order to preserve the continuity of $\delta B(z)$ as a function of z, it is assumed that the field error $\delta B_n(z)$ associated with the n^{th} pole pair extends over the region $z_n - \lambda_w/4 < z < z_n + \lambda_w/4$, such that $|\delta B_n(z)|$ is maximum at $z = z_n$ and is zero at $z = z_n \pm \lambda_w/4$. For simplicity, the following functional forms are chosen for the field errors of the n^{th} pole pairs in the x– and y–directions:

$$\delta B_{nx}(z) = \begin{cases} \Delta B_x \epsilon_{nx} \cos k_w z, & \text{if } |z - z_{nx}| < \lambda_w/4; \\ 0, & \text{otherwise,} \end{cases} \quad (37a)$$

$$\delta B_{ny}(z) = \begin{cases} \Delta B_y \epsilon_{ny} \sin k_w z, & \text{if } |z - z_{ny}| < \lambda_w/4; \\ 0, & \text{otherwise.} \end{cases} \quad (37b)$$

Here, ΔB_x and ΔB_y are the maximum field errors for the wiggler in the x– and y–directions; and the centers of the pole pairs in the x– and y–directions, z_{nx} and z_{ny},

are given by $z_{nx} = (n-1)\lambda_w/2$ and $z_{ny} = (n-1/2)\lambda_w/2$. Also, ϵ_{nx} (or ϵ_{ny}) is a random number between -1 and 1 which is constant over the region $|z - z_{nx}| < \lambda_w/4$ (or $|z - z_{ny}| < \lambda_w/4$) and is uncorrelated with the value of ϵ_{mx} (or ϵ_{my}) for $m \neq n$. Furthermore, it is assumed that the statistical distributions for ϵ_{nx} (or ϵ_{ny}) are identical for each pole pair (all n). The distribution for ϵ_n is chosen to be uniform from -1 to 1 such that $\langle\epsilon_{nx}^2\rangle = \langle\epsilon_{ny}^2\rangle = 1/3$, although any random distribution with zero mean and finite variance would be equally satisfactory. This model for the field errors δB_y is essentially identical to that used by Kincaid,[3] only Kincaid assumed the random coefficients ϵ_{ny} to be Gaussian distributed. A schematic of this field error model is shown in Fig. 2.

To compare the above numerical model for $\delta B(z)$ to the analytical model which assumes $\delta B(z)$ to be a random, homogeneous variable with autocorrelation length z_c, it is necessary to calculate the correlation function $\langle\delta B(z)\delta B(z+\Delta z)\rangle$ for the numerical model. Recall that the analytical theory assumed $\delta B(z)$ to be homogeneous such that $\langle\delta B(z)\delta B(z+\Delta z)\rangle$ is a function only of Δz. For the numerical model, however, this is not the case since $\delta B(z)$ was chosen to have a $\cos k_w z$ (or $\sin k_x z$) dependence over a given pole pair. Hence, a comparison of the numerical model with the analytic theory requires that the expression for the numerical model of $\langle\delta B(z)\delta B(z+\Delta z)\rangle$ be spatially averaged over a wiggler period. Doing this, one finds for the numerical model,[3]

$$\begin{aligned}\langle\delta B_x(z)\delta B_x(z+\Delta z)\rangle = \frac{1}{2}\Delta B_x^2\left\langle\epsilon_x^2\right\rangle\Bigg[&\left(1-\frac{2|\Delta z|}{\lambda_w}\right)\cos k_x\Delta z \\ &+\frac{1}{\pi}\sin k_w|\Delta z|\Bigg],\ \text{for } |\Delta z| < \frac{\lambda_w}{2},\end{aligned} \tag{38}$$

and zero otherwise (along with the corresponding expression for the field error correlation in the y–direction). Using the definition for the autocorrelation length z_c given in Sec. II, one identifies that for the numerical model

$$\left\langle\delta B_x^2\right\rangle = \frac{1}{2}\Delta B_x^2\left\langle\epsilon_x^2\right\rangle = \frac{1}{6}\Delta B_x^2, \tag{39a}$$

$$\left\langle\delta B_y^2\right\rangle = \frac{1}{2}\Delta B_y^2\left\langle\epsilon_y^2\right\rangle = \frac{1}{6}\Delta B_y^2, \tag{39b}$$

and

$$z_{cx} = z_{cy} = \frac{4}{\pi^2}\lambda_w. \tag{39c}$$

In the above expressions for $\langle\delta B^2\rangle$, the factors of 1/2 arise from the spatial average of $\cos^2 k_x z$ and $\sin^2 k_w z$. Hence, the numerical model gives an rms field error of $\langle\delta B^2\rangle^{1/2} = \Delta B/\sqrt{6}$, where ΔB is the maximum field error of the wiggler ensemble, and an autocorrelation length equal to $4\lambda_w/\pi^2$.

The above model for the wiggler errors was used in the numerical code to simulate electron beam propagation in a helical wiggler. A particular realization of a wiggler was obtained for a given single set of random field error parameters ϵ_{nx} and ϵ_{ny}. For such an individual realization, various properties of the electron beam were calculated such as the transverse displacement of the beam centroid and the variation of the electron beam parallel energy. These beam quantities were obtained by averaging the appropriate quantities for the individual electrons over the distribution of electrons within the beam. Ensemble averages of a beam quantity were then obtained by averaging the beam quantity over 40 individual wiggler realizations (40 sets of 800 distinct random field error parameters ϵ_{nx} and ϵ_{ny}). The runs described below are for a helical wiggler of length $L = 40$ m, with $B_w = 4.3$ kG, $\lambda_w = 5.0$ cm, and $\langle \delta B^2 \rangle^{1/2} / B_w = 0.3\%$; and for an electron beam of energy $\gamma = 270$, with radius $r_b = 0.08$ cm and a normalized emittance of 11.3 mrad–cm, which matches the acceptance of the transport channel. These parameters give $a_w = 2$ and $k_\beta = 9.5$ m.

A typical transverse orbit $\delta x(z)$ occurring in a single wiggler realization is shown for a case without transverse focusing in Fig. 3 and for a case with transverse focusing in Fig. 4. Figure 3 shows a large 1-D orbit displacement of 6.7 cm, whereas transverse focusing leads to oscillations about the axis at the betatron wavelength with a maximum displacement of 0.45 cm, as is shown in Fig. 4. Similarly, the parallel energy $\gamma_\parallel(z)$ for a typical wiggler realization is shown for a case without transverse focusing in Fig. 5 and for a case with transverse focusing in Fig. 6. Figure 5 shows, in the 1-D limit, a 2.5% increase in the parallel beam energy. This is in agreement with Eq. (15a) which indicates an increase in the mean parallel energy provided $a_w^2 > 2$. Figure 6 shows a decrease in the parallel energy of about 5%, which is in agreement with Eq. (15b) which indicates that transverse focusing will lead to a decrease in the mean parallel energy. Notice also that the parallel energy in Fig. 6 exhibits oscillations at 1/2 the betatron wavelength. This reflects the fact that $\gamma_\parallel$ depends on terms proportional to $\delta\beta_\perp^2$ as indicated by Eq. (13).

The rms transverse displacement of the beam centroid $\langle \delta x^2(z) \rangle^{1/2}$ as obtained from performing the ensemble average numerically is shown in Fig. 7 (solid curve), along with the theoretical result (dashed curve), for the case without transverse focusing. The theory and simulation are in good agreement showing a maximum rms displacement of about 5 cm. Figure 8 plots the rms beam centroid displacement for the case including transverse focusing, showing the comparison between the numerically obtained ensemble average (solid curve) and the theoretical result (dashed curve). Both curves exhibit oscillations at 1/2 the betatron wavelength and show a maximum rms displacement of about 0.25 cm.

The remaining plots describe the parallel energy $\gamma_{\parallel}$ of the electron beam. The normalized ensemble averaged energy $\langle\gamma_{\parallel}\rangle/\gamma_{\parallel 0} - 1$ is shown in Figs. 9 and 10 for the cases without and with transverse focusing, respectively, comparing the simulation (solid curve) and the analytical theory (dashed curve). Notice that in the absence of focusing Fig. 9 shows an increase (of about 1.3%) in the mean parallel energy whereas Fig. 10, which includes focusing, shows a decrease (of about 3.5%) in the mean parallel energy. This is in agreement with the theory for the case $a_w = 2$. Similarly, the normalized variance $\hat{\sigma}_{\parallel} \equiv (\langle\gamma_{\parallel}^2\rangle - \langle\gamma_{\parallel}\rangle^2)^{1/2}/\gamma_{\parallel 0}$ is shown in Figs. 11 and 12 for the cases without and with transverse focusing, respectively, comparing the simulation (solid curve) and the analytical theory (dashed curve). In both Figs. 11 and 12 the variance in the parallel energy is quite large, becoming greater than 10% in less than 20 m.

These simulation results indicate that the analytical theory gives a good approximation to the qualitative and quantitative behavior of the electron beam. Several differences which appear between the theory and the simulations may be attributed to the following physical and numerical effects. The electron beam in the simulation has a finite emittance and beam cross–section. This results in a mean–square transverse position which is non–zero initially. This is seen in Figs. 3, 4, 7 and 8. For cases in which weak focusing is included, betatron oscillations occur in the beam motion. Since the simulations include finite beam emittance, one expects the amplitude of these oscillations to be larger than the predictions of the analytic theory. This is the case in Figs. 8, 10 and 12. Also, the amplitude of this oscillation in the simulations is not constant as the beam propagates . This effect is due to the finite sampling size used in performing the ensemble average. In principle, an infinite set of wigglers is needed in order to replicate the smooth functional dependence of the theoretical ensemble average. For the ensemble average of variables whose variance is large, the sampling size used must be large in order to recover the smooth functional dependence. This is seen in the simulations shown in Figs. 9–12, in which various statistical moments of the parallel beam energy are plotted. These ensemble averages were performed over a set of 40 realizations, hence, these plots do not exhibit smooth behavior.

VII. Discussion

The above analysis indicates that intrinsic magnetic field errors perturb electron beam propagation through the wiggler and lead to various undesirable effects such as a random walk of the electron beam centroid[3-6] as well as fluctuations in the parallel electron energy of the beam.[6] These detrimental effects were studied both analytically and numerically. The analytical treatment assumed that the motion of the electron beam could be adequately approximated by a single particle located at the beam centroid. Expressions were derived for the centroid motion for a single wiggler realization (a particular occurrence of random errors δB) as well as for averages taken over an ensemble of wigglers having the same statistical properties. The field errors δB were assumed to be random, homogeneous functions of the propagation distance z with zero mean and with a finite variance. The transverse dependence of δB was neglected assuming that the variation in δB was small over the transverse extent of the electron beam. Beam propagation was studied through both helical and planar wiggler configurations, with and without transverse focusing. The results of the analytical theory were then supported by performing 3-D particle simulations of electron beam transport including the effects of finite emittance and space charge. The results of these simulations showed good agreement with the analytic theory.

Physically, as the electrons propagated through the wiggler, they experienced random $\mathbf{v}_z \times \delta\mathbf{B}$ forces which led to a random transverse walk of the beam centroid. In the absence of transverse focousing, the rms value of the centroid displacement scale as $\langle \delta x^2 \rangle^{1/2} \sim z^{3/2}$, which is in agreement with the results of Kincaid[3]. More specifically, the transverse displacement for a single wiggler realization is given by Eq. (10) and the mean–square value averaged over the wiggler ensemble is given by Eq. (11). Transverse focusing, however, impedes the random walk such that $\langle \delta x^2 \rangle^{1/2} \sim z^{1/2}$ in the large z limit, $(2k_\beta z)^2 >> 1$, which is in agreement with the results of Elliott and McVey[4] as well as Shay and Scharlemann.[5] Expressions for a single realization and for the ensemble averaged mean–square of the centroid displacement with transverse focusing are given by Eqs. (21) and (24). In the limit $(2k_\beta z)^2 >> 1$, the rms centroid displacement can be written as $\langle \delta x^2 \rangle^{1/2}/\lambda_w \simeq \langle \delta B^2/B_w^2 \rangle^{1/2}(N/2)^{1/2}$, where $N = z/\lambda_w$ is the number of wiggler periods the electron beam has traveled and where $z_c \simeq \lambda_w/2$ has been assumed. For example, $\langle \delta B^2/B_w^2 \rangle^{1/2} = 0.1\%$ and $N = 200$ gives $\langle \delta x^2 \rangle^{1/2}/\lambda_w \simeq 10^{-2}$.

This random transverse motion of the beam centroid leads to variations in the parallel beam energy[6] through conservation of energy. The above analysis indicates that both the

mean and the square of the variance of the parallel energy variation scale linearly with z, with or without transverse focusing (i.e., transverse focusing does not significantly reduce the parallel energy deviation). The expression for the parallel beam energy for a single wiggler realization is given by Eq. (13) along with the appropriate expressions for $\delta\beta$ (such as Eq. (22) for the case of a helical wiggler with transverse focusing). Expressions for the ensemble averages of the parallel energy are given by Eqs. (26) and (27) for the helical case. In the limit $(2k_\beta z)^2 >> 1$, then the normalized variance of the parallel beam energy $\hat{\sigma}_\| \equiv (\langle\gamma_\|^2\rangle - \langle\gamma_\|\rangle^2)^{1/2}/\gamma_{\|0}$ can be written as $\hat{\sigma}_\| \simeq \pi\langle\delta B^2/B_w^2\rangle^{1/2}N^{1/2}$, where $a_w^2 >> 1$ has been assumed. For example, $\langle\delta B^2/B_w^2\rangle^{1/2} = 0.1\%$ and $N = 100$ gives $\hat{\sigma}_\| \simeq 3 \times 10^{-2}$.

These effects may degrade FEL performance. For example, the random walk of the electron beam centroid may become too large over a sufficiently short distance such that the radiation beam is no longer optically guided.[7] When this occurs, the electron beam centroid no longer overlaps the centroid of the radiation beam, thus leading to a loss of the FEL interaction and loss of FEL gain. Ideally, it may be desirable to keep the magnitude of the transverse beam displacement less than the beam radius $|\delta x|/r_b < 1$ in order to avoid such detrimental effects. Alternatively, the parallel energy variation induced by the wiggler field errors may become sufficiently large so as to destroy the FEL resonant interaction. Statistically speaking, one can interpret the parallel energy variation due to field errors as an effective energy spread which increases with increasing axial distance. As discussed above, $\hat{\sigma}_\| \sim z^{1/2}$ and for rms random field errors of 0.1%, then after 100 wiggler periods there exists an effective energy spread of $\hat{\sigma}_\| \simeq 1.0\%$, which is a significant amount. In order to avoid loss of the FEL resonance, it is necessary for the parallel energy spread to be small compared to the intrinsic power efficiency η for FELs in the low gain or high gain regimes,[8] $\hat{\sigma}_\| < \eta$. In the trapped particle regime, the parallel energy spread needs to be small compared to the width of the FEL ponderomotive potential[9] Φ_p, which implies $\hat{\sigma}_\| < |e\Phi_p|/(\gamma m_0 c^2)$. For example, in the low gain regime $\eta = 1/(2N)$ which implies that the rms field errors must be less than $\langle\delta B^2/B_w^2\rangle^{1/2} < 1/(2\pi N^{3/2})$, where the expression for $\hat{\sigma}_\|$ given in the previous paragraph has been used. For $N = 100$, this implies that in the low gain regime $\langle\delta B^2/B_w^2\rangle^{1/2} < 2 \times 10^{-4}$, which may be difficult to achieve in practice.

In an actual wiggler magnet, however, the field errors $\delta B(z)$ are not entirely random functions of z. In practice, once the field errors from each individual magnet pole have been measured, one may be clever in how these poles are then arranged during the assembly of the wiggler such that the detrimental effects of these field errors are minimized.[15] For example, if the field error from a given pole pair tends to deflect the electron beam in a given direction, then the next pole pair should be chosen such that it deflects the electron

beam in the opposite direction so as to keep the beam as close to axis as possible. A typical figure of merit used in practice is the line integral of the field errors $|\int dz'\delta B(z')|$ which is to be minimized during wiggler assembly. If the magnitude of the centroid displacement is to be minimized, however, then the above analysis indicates that the pole arrangement should be chosen to minimize the integral $|\int dz' \sin k_\beta(z'-z)\delta B(z')|$, as is shown by Eq. (21). In some FEL applications it may be the case that the reduction in gain resulting from finite field errors is dominated by the parallel energy deviation as opposed to the random walk of the electron beam centroid. In such cases it may be desirable to arrange the magnet poles such that the expression for the magnitude of the parallel energy deviation is minimized, $|\delta\gamma_\parallel| \equiv |\gamma_\parallel - \gamma_{\parallel 0}|$, where $\gamma_\parallel$ is given by Eq. (13) along with the appropriate expressions for $\delta\beta_\perp$. Preliminary analysis by the authors suggests that if one wishes to maximize the FEL gain, then the magnet poles should be arranged such that the magnitude of the deviation in the relative phase of the electrons in the ponderomotive wave $|\delta\psi|$ is minimized, where $\delta\psi \sim \int dz'\delta\gamma_\parallel$. Notice that the centroid displacement scales as $\delta x \sim \int dz'\delta\beta_\perp$, whereas the relative phase deviation $\delta\psi$ depends on terms of the form $\int dz'\beta_{\perp 0}\delta\beta_\perp$ and of the form $\int dz'\delta\beta_\perp^2$. Hence, minimization of δx does not necessarily correspond to minimization of of $\delta\psi$.

External steering coils may also be used to reduce the detrimental effects of field errors.[3-5] For example, steering coils may be used to periodically steer the electron beam back on axis and thus prevent the beam centroid displacement from becoming too large. Although the random walk of the centroid may be greatly reduced in this way, it is not clear that this will also greatly reduce the parallel energy variation $\delta\gamma_\parallel$ or, more importantly, the relative phase deviation $\delta\psi$. Preliminary analysis by the authors indicates that if external coils are used to steer the electron beam back on axis after a given distance l, such that $\delta x(l) = 0$, then the mean value of the relative phase deviation $\langle\delta\psi(l)\rangle$ is only reduced by a factor of three, i.e., 1/3 times the value in the absence of external beam steering. A more complete analysis of the effects of field errors on FEL gain, including the effects of beam steering, is currently being pursued by the authors and will be the subject of future publications.

Acknowledgements

The authors would like to acknowledge useful discussions with P. Sprangle. This work was supported by the Office of Naval Research, Contract No. N00014-87-f-0066, through the National Institute of Standards and Technology; and by the U.S. Department of Energy.

References

1) See, for example, *Free Electron Lasers, Proceedings of the 9th International FEL Conference*, ed. by P. Sprangle, C.M. Tang and J. Walsh (North–Holland, Amsterdam, 1988).

2) K.E. Robinson, D.C. Quimby, J.M. Slater, T.L. Churchill and A.S. Valla, in *Free Electron Lasers, Proceedings of the 8th International FEL Conference*, ed. by M.W. Poole (North–Holland, Amsterdam, 1987), p. 62; K.E. Robinson, D.C. Quimby and J.M. Slater, IEEE J. Quantum Electron. QE-23, 1497 (1987).

3) B.M. Kincaid, J. Opt. Soc. Am. B **2**, 1294 (1985).

4) C.J. Elliott and B.D. McVey, in *World Scientific Proceedings of Undulator Magnets for Synchrotron Radiation and Free Electron Lasers*, Trieste, Italy, June 1987.

5) H.D. Shay and E.T. Scharlemann, in *Free Electron Lasers, Proceedings of the 9th International FEL Conference*, ed. by P. Sprangle, C.M. Tang and J. Walsh (North–Holland, Amsterdam, 1988), p. 601.

6) C.M. Tang, E. Esarey, W. Marable and P. Sprangle, presented at the 9th International FEL Conference, Williamsburg, VA, Sept. 14-16, 1987; also presented at the Workshop for Advanced Wigglers, Los Alamos, NM, Dec. 3, 1987; E. Esarey, W. Marable, C.M. Tang and P. Sprangle, Bull. Amer. Phys. Soc. **33** (4), 1066 (1988).

7) P. Sprangle, A. Ting and C.M. Tang, Phys. Rev. Lett. **59**, 202 (1987); Phys. Rev. A **36**, 2773 (1987); in *Free Electron Lasers, Proceedings of the 8th International FEL Conference*, ed. by M.W. Poole (North–Holland, Amsterdam, 1987), p. 136.

8) P. Sprangle, R.A. Smith and V.L. Granatstein, in *Infrared and Millimeter Waves*, ed. by K. Button (Academic, New York, 1979), Vol. I, p. 279; P. Sprangle, C.M. Tang and C.W. Roberson, Nucl. Instrum. Methods A **239**, 1 (1985).

9) P. Sprangle and C.M. Tang, Appl. Phys. Lett. **39**, 677 (1981); C.M. Tang and P. Sprangle, in *Free-Electron Generation of Coherent Radiation, Physics of Quantum Electronics*, ed. by S.F. Jacobs, G.T. Moore, H.S. Pilloff, M. Sargent III, M.O. Scully and R. Spitzer (Addison–Wesley, Reading, MA, 1982), Vol. 9, p. 627.

10) W. Marable, C.M. Tang and P. Sprangle, Bull. Amer. Phys. Soc. **32** (9), 1794 (1987).

11) See, for example, *Basic Principles of Plasma Physics: A Statistical Approach*, S. Ichimaru (Benjamin–Cummings, Reading, MA, 1973), p. 237.

12) See, for example, *Stochastic Processes in Physics and Chemistry*, N.G. Van Kampen (North–Holland, Amsterdam, 1981), p. 223.

13) P. Diament, Phys. Rev. A **23**, 2737 (1981); T.I. Smith and J.M.J. Madey, Appl. Phys. B **27**, 195 (1982).

14) W.M. Fawley, D. Prosnitz and E.T. Scharlemann, Phys. Rev. A **30**, 2472 (1987).

15) M.S. Curtin, A. Bhowmik, W.A. McMullin, S.V. Benson, J.M.J. Madey, B.A. Richman and L. Vintro, in *Free Electron Lasers, Proceedings of the 9th International FEL Conference*, ed. by P. Sprangle, C.M. Tang and J. Walsh (North–Holland, Amsterdam, 1988), p. 91.

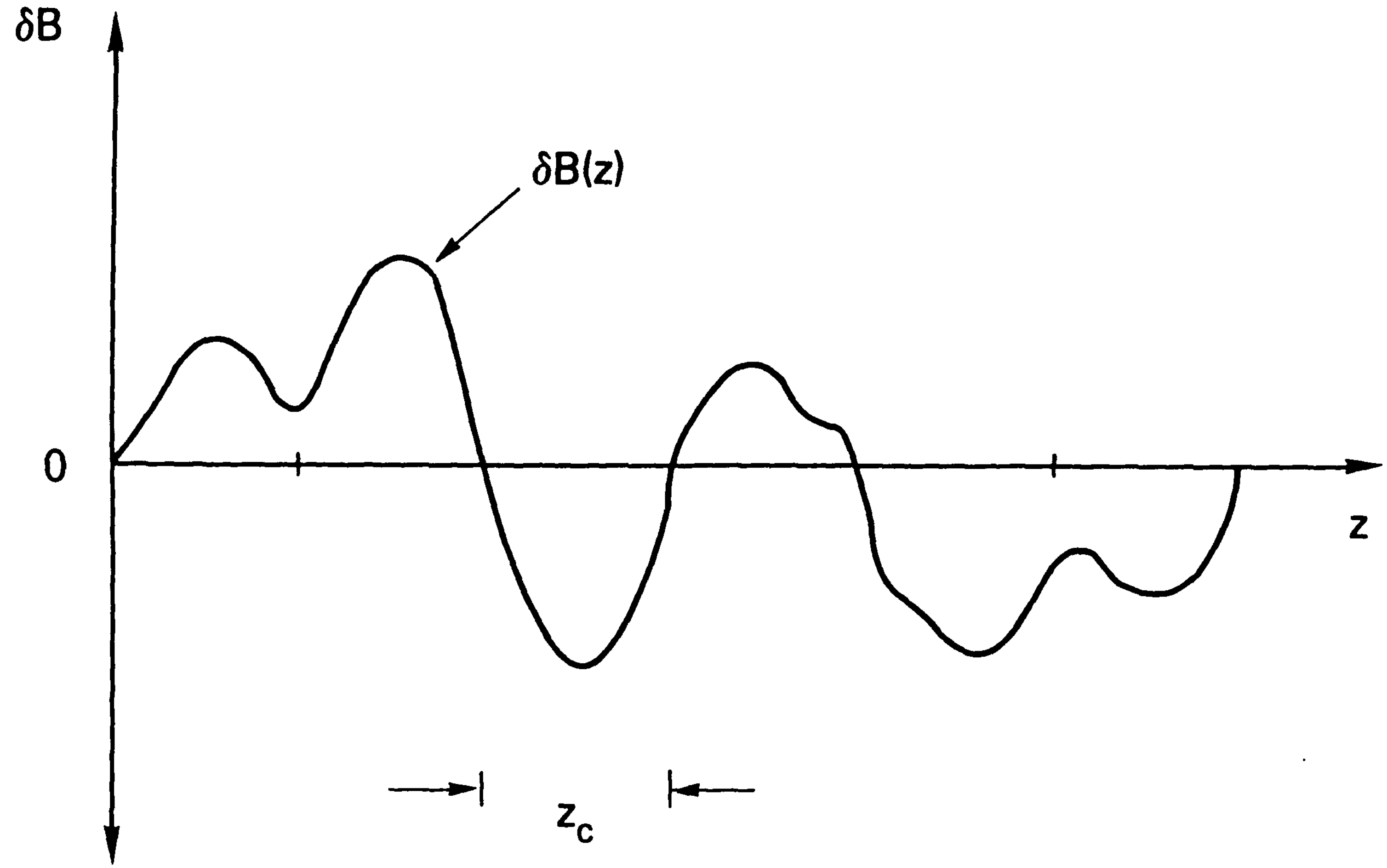

FIG. 1. Schematic of random homogeneous field errors $\delta B(z)$ which have a zero mean, a finite variance $\langle \delta B^2 \rangle^{1/2}$ and a finite autocorrelation distance $z_c \simeq \lambda_w/2$.

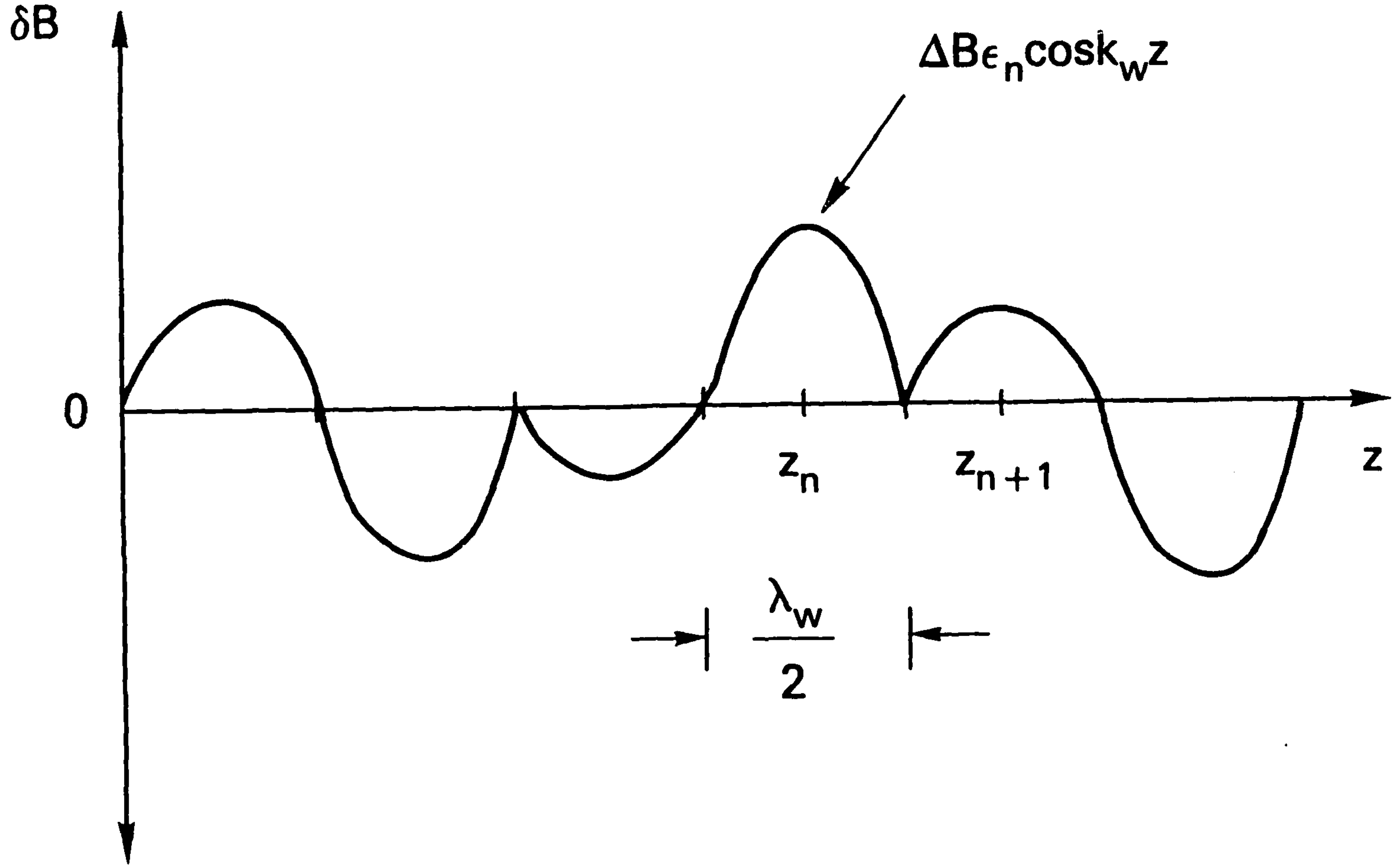

FIG. 2. Schematic of the random field error model used in the numerical simulations in which the axial dependence of $\delta B(z)$ for a given pole pair is sinusoidal and extends over a distance $\lambda_w/2$.

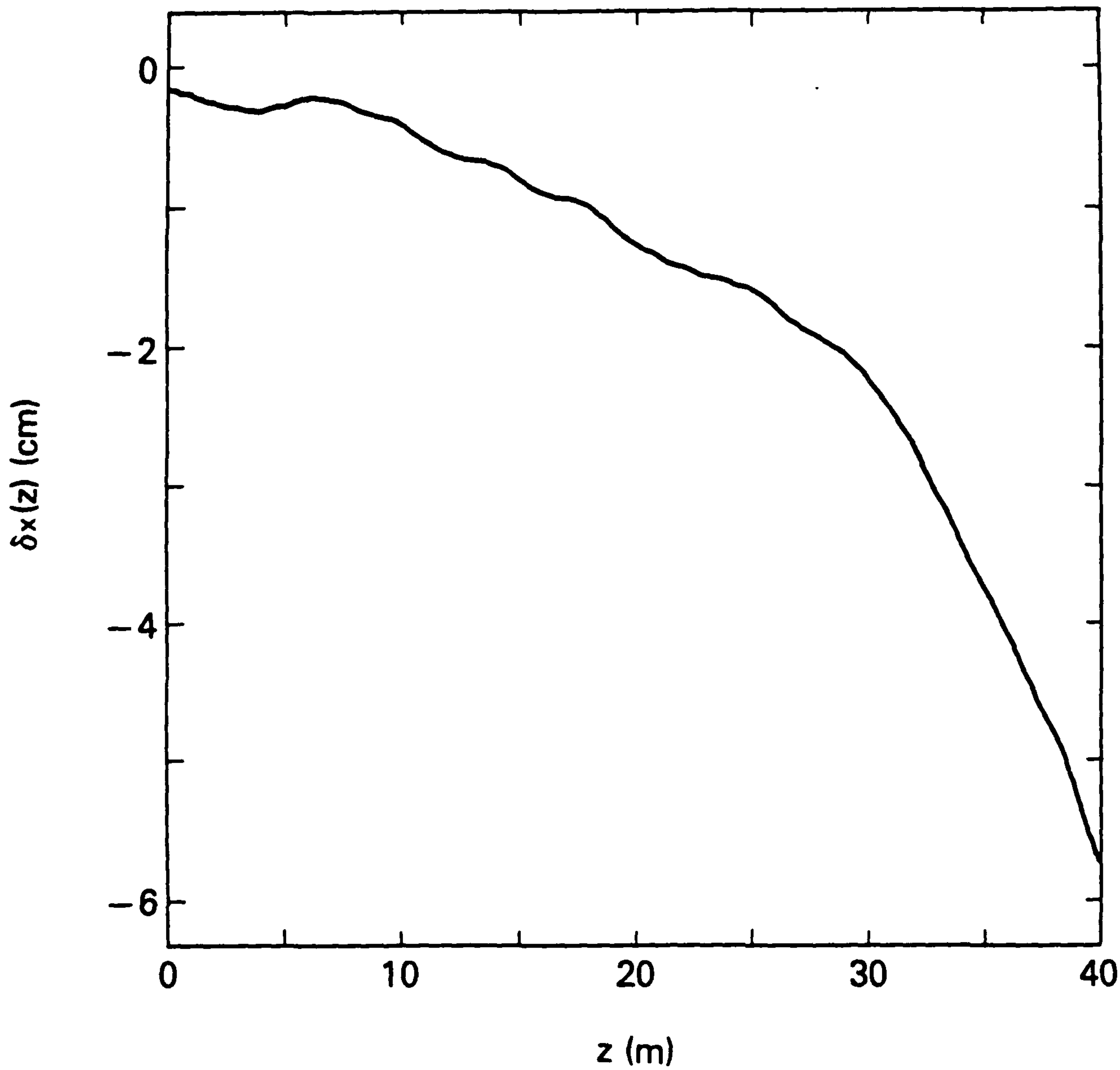

FIG. 3. A typical transverse orbit occurring in a single wiggler realization without transverse focusing for the parameters $\gamma = 270$, $a_w = 2$, $\lambda_w = 5$ cm and $\langle \delta B_w^2 \rangle^{1/2} / B_w = 0.3\%$.

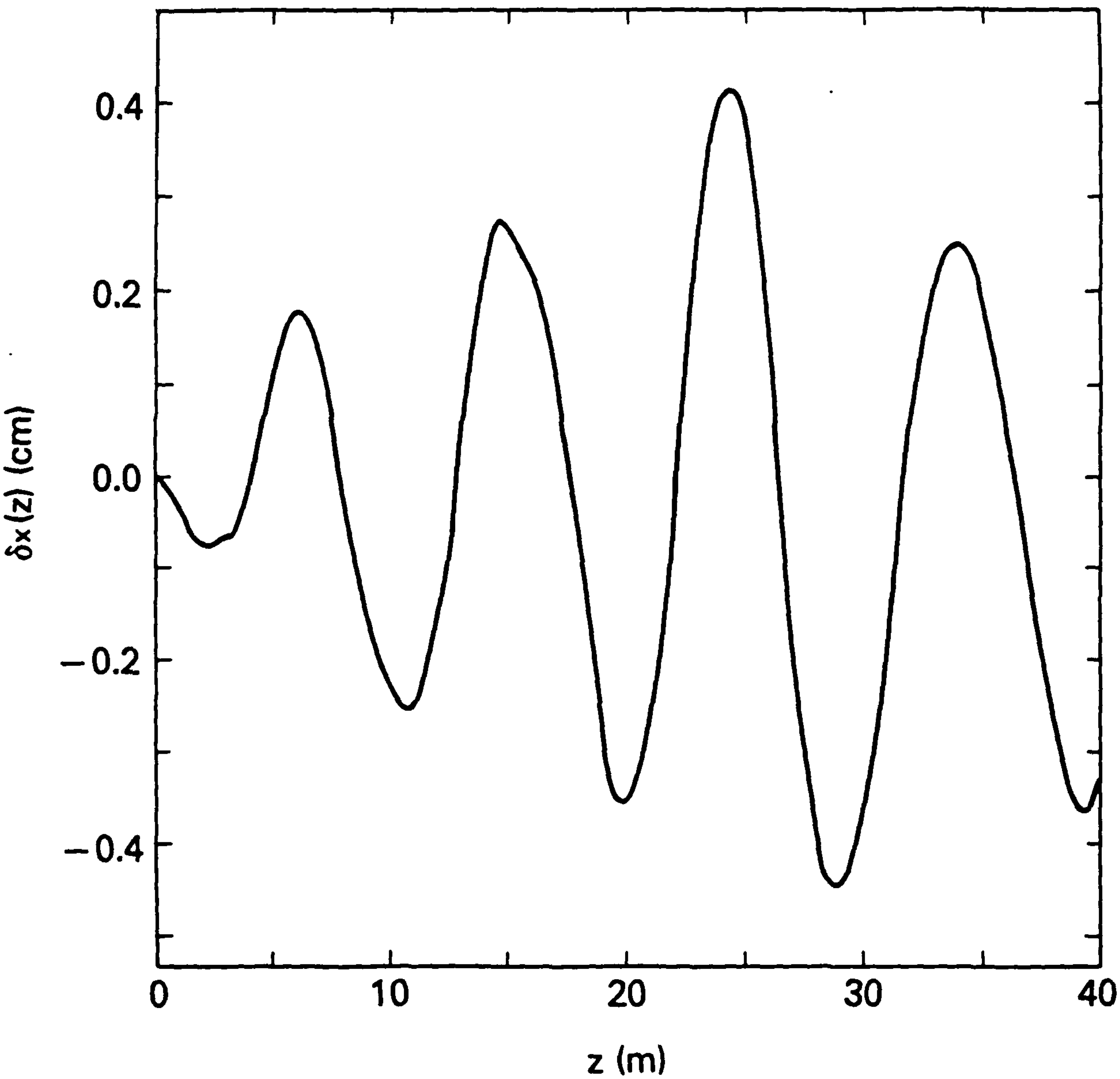

FIG. 4. A typical transverse orbit occurring in a single wiggler realization with transverse focusing for the parameters $\gamma = 270$, $a_w = 2$, $\lambda_w = 5$ cm and $\langle \delta B_w^2 \rangle^{1/2} / B_w = 0.3\%$.

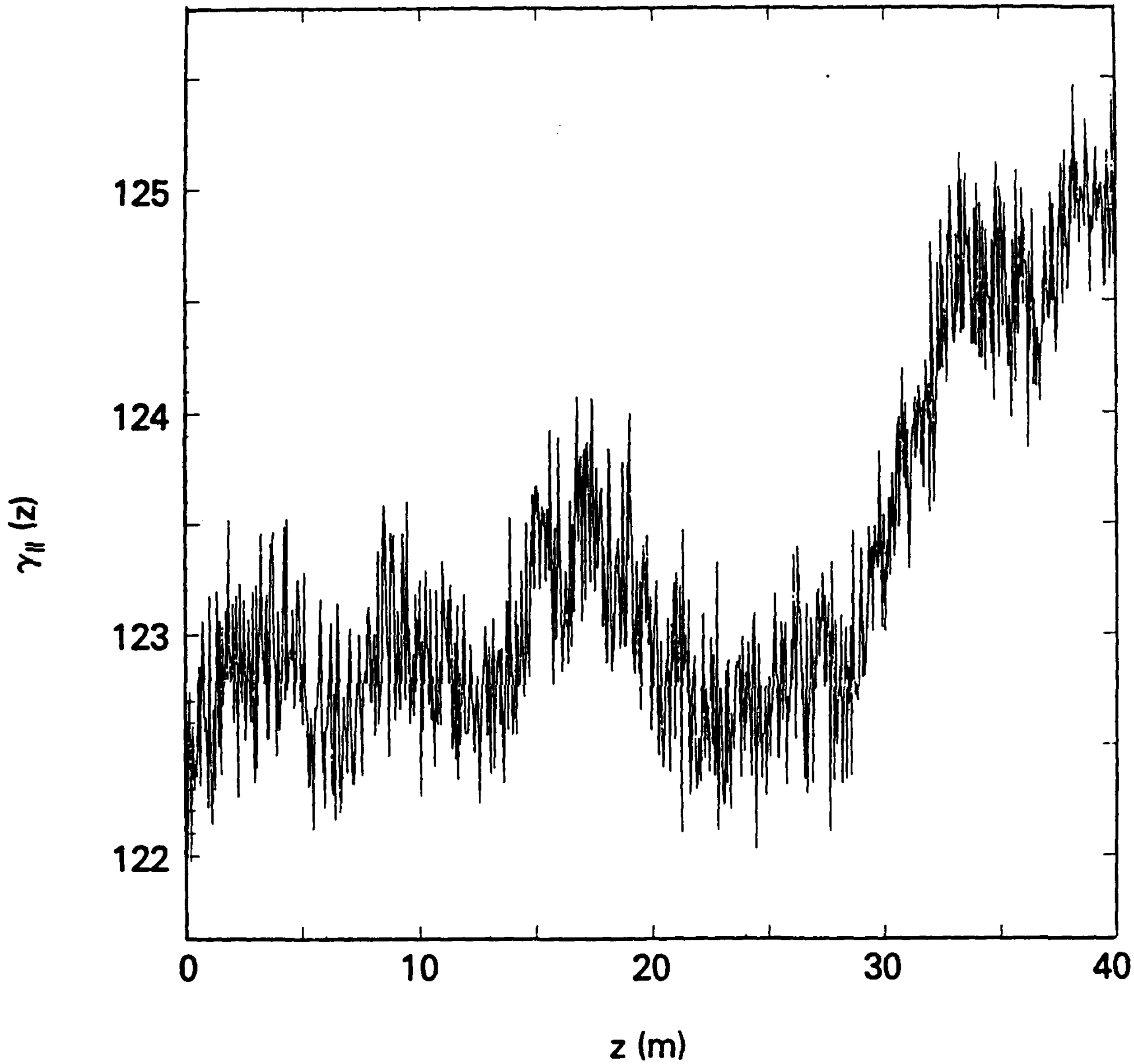

FIG. 5. The parallel beam energy for a single wiggler realization without transverse focusing for the parameters $\gamma = 270$, $a_w = 2$, $\lambda_w = 5$ cm and $\langle \delta B_w^2 \rangle^{1/2} / B_w = 0.3\%$.

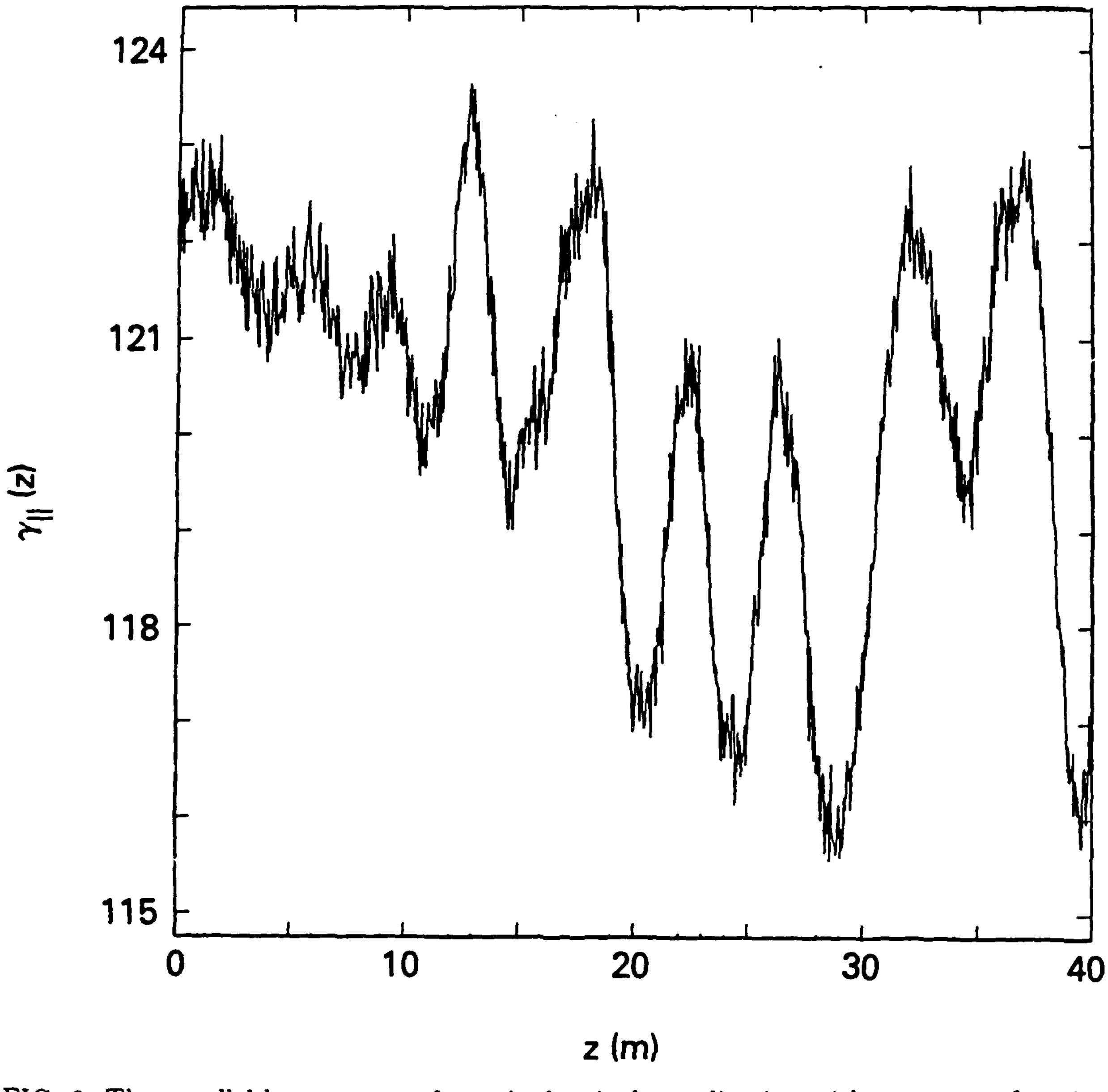

FIG. 6. The parallel beam energy for a single wiggler realization with transverse focusing for the parameters $\gamma = 270$, $a_w = 2$, $\lambda_w = 5$ cm and $\langle \delta B_w^2 \rangle^{1/2} / B_w = 0.3\%$.

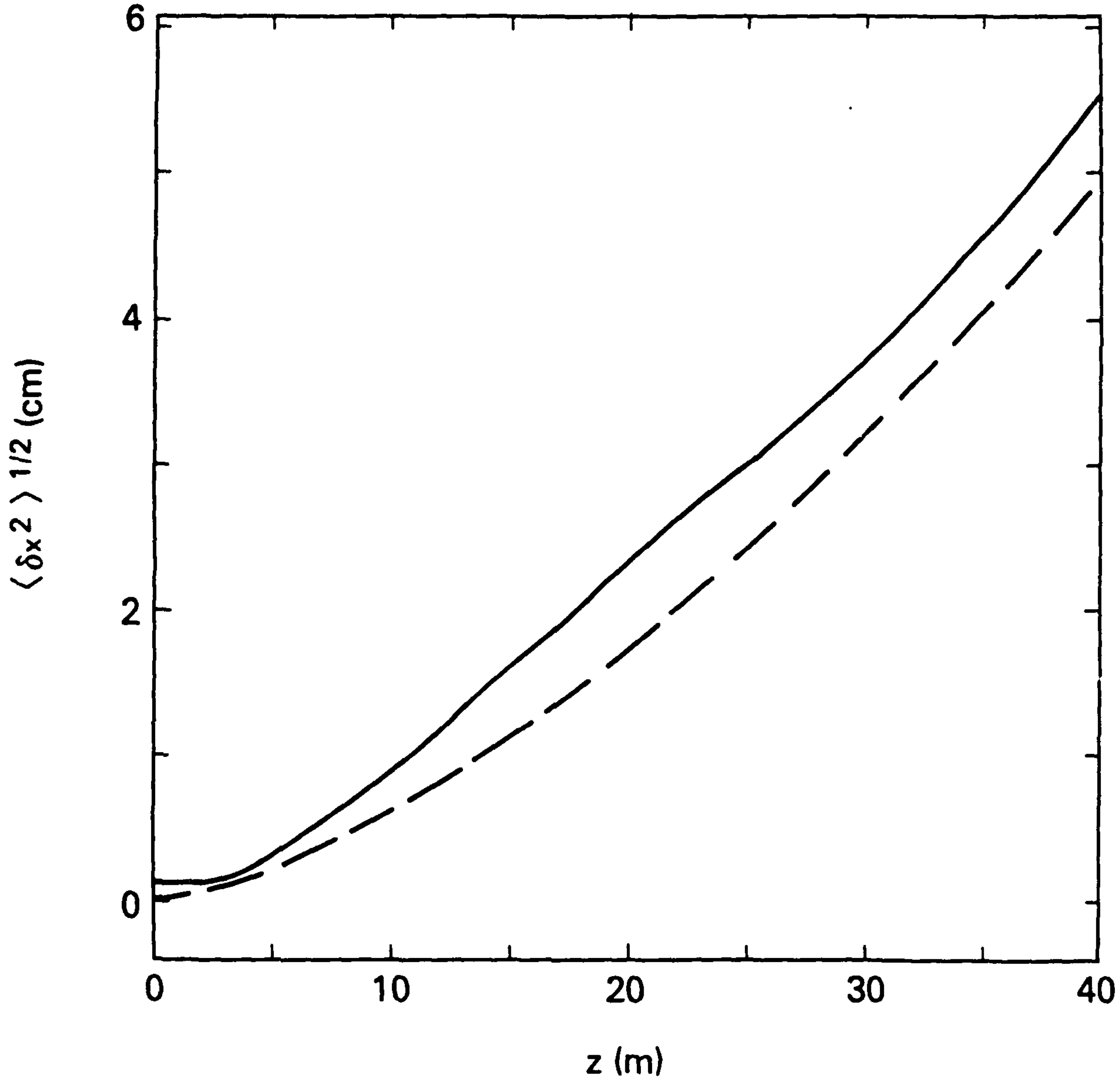

FIG. 7. The rms transverse displacement of the beam centroid as obtained from simulation (solid curve) and from theory (dashed curve) for the case without transverse focusing ($\gamma = 270$, $a_w = 2$, $\lambda_w = 5$ cm and $\langle \delta B_w^2 \rangle^{1/2} / B_w = 0.3\%$).

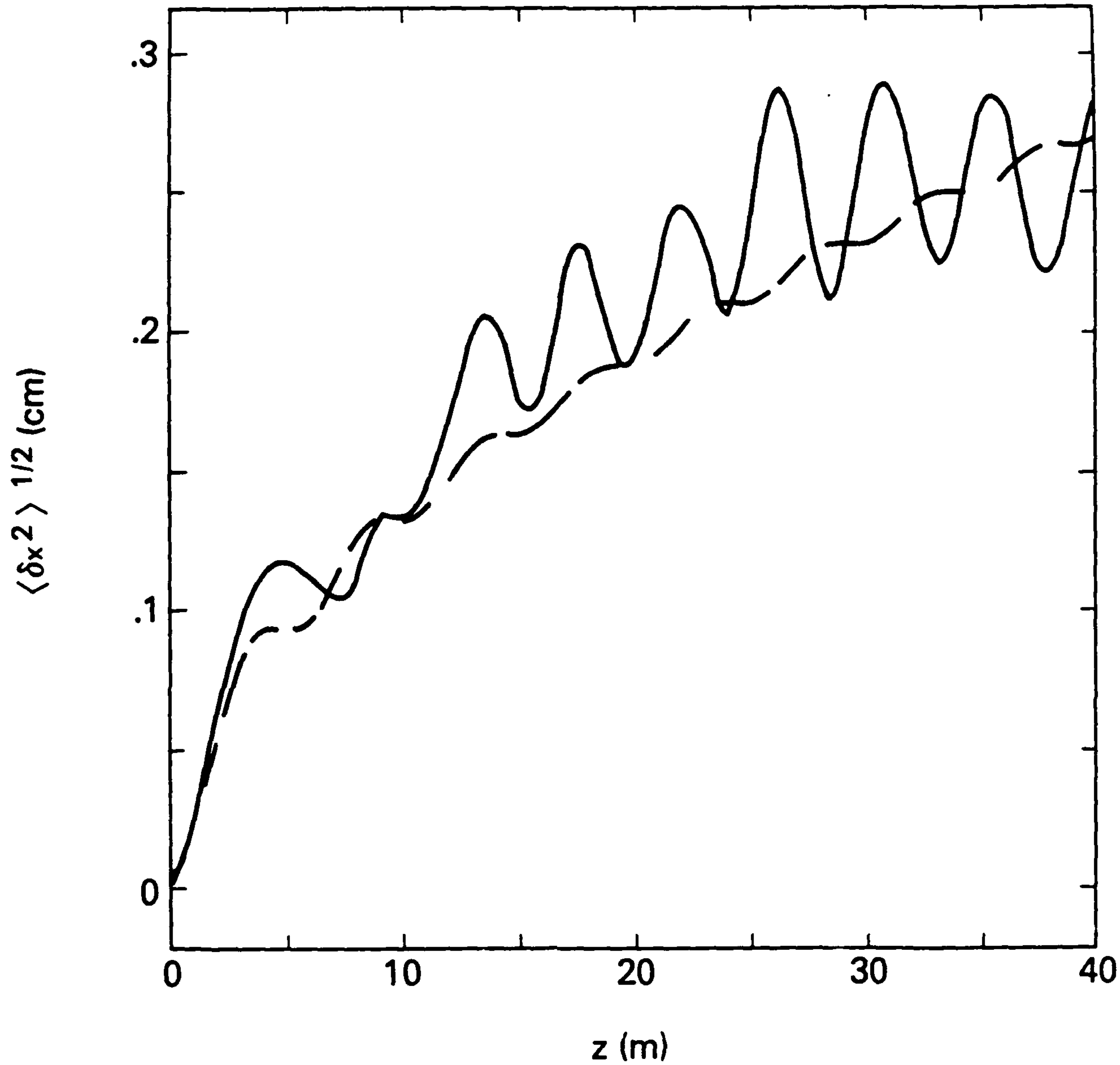

FIG. 8. The rms transverse displacement of the beam centroid as obtained from simulation (solid curve) and from theory (dashed curve) for the case with transverse focusing (γ = 270, $a_w = 2$, $\lambda_w = 5$ cm and $\langle \delta B_w^2 \rangle^{1/2} / B_w = 0.3\%$).

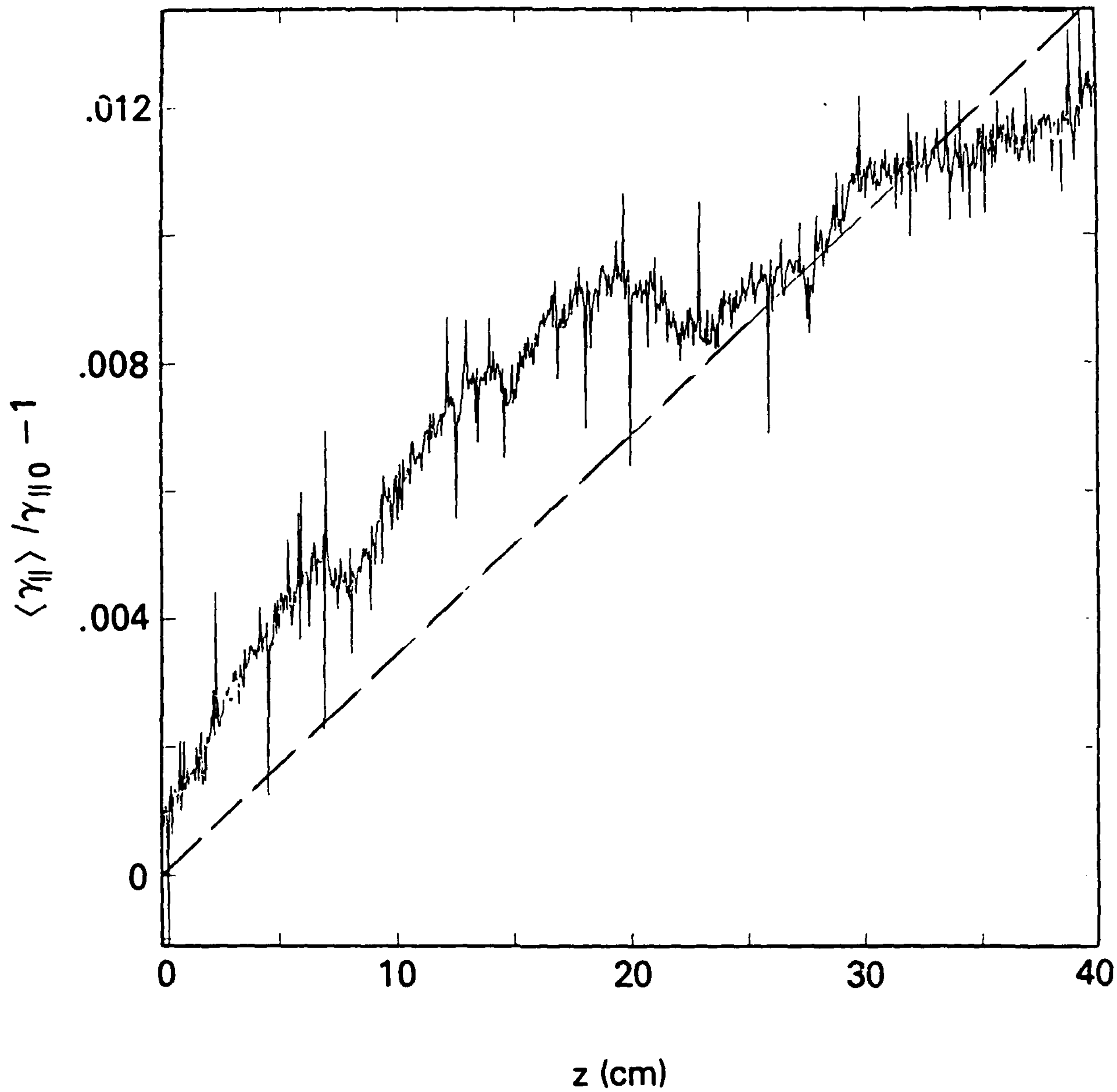

FIG. 9. The normalized mean parallel energy $\langle \gamma_{\parallel} \rangle / \gamma_{\parallel 0} - 1$ as obtained from simulation (solid curve) and from theory (dashed curve) for the case without transverse focusing ($\gamma = 270$, $a_w = 2$, $\lambda_w = 5$ cm and $\langle \delta B_w^2 \rangle^{1/2} / B_w = 0.3\%$).

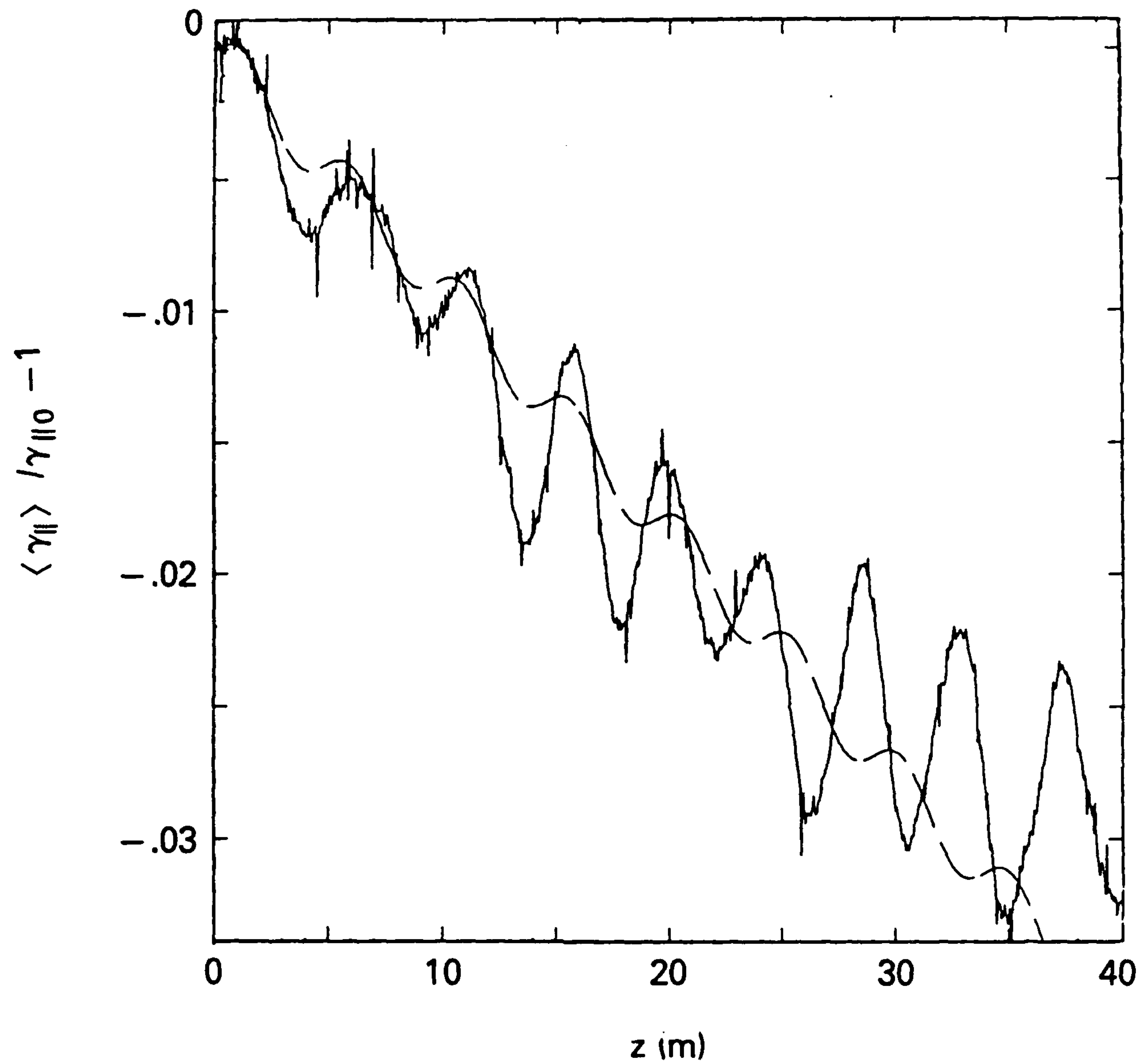

FIG. 10. The normalized mean parallel energy $\langle \gamma_{\|} \rangle / \gamma_{\|0} - 1$ as obtained from simulation (solid curve) and from theory (dashed curve) for the case with transverse focusing (γ = 270, $a_w = 2$, $\lambda_w = 5$ cm and $\langle \delta B_w^2 \rangle^{1/2} / B_w = 0.3\%$).

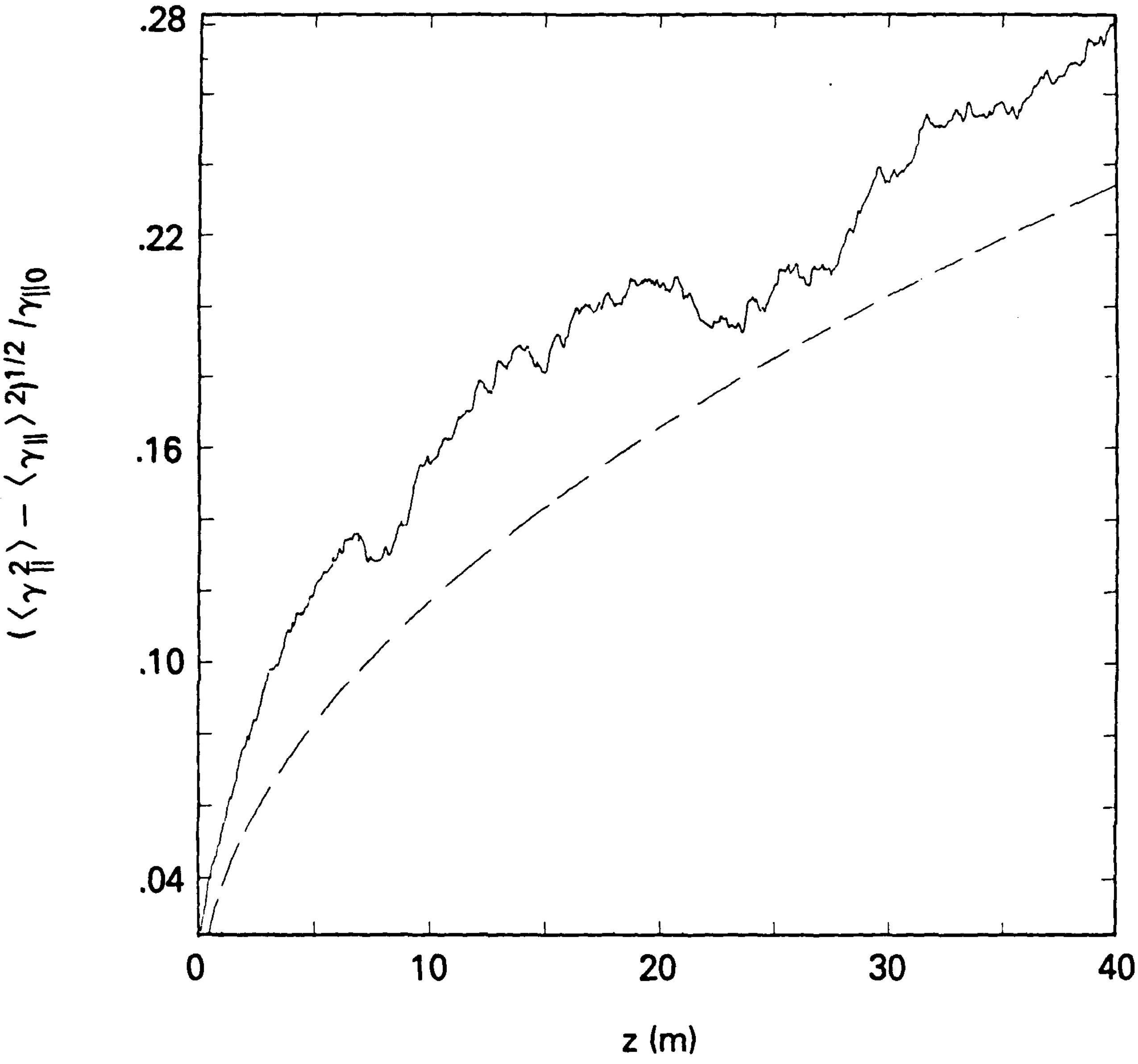

FIG. 11. The normalized variance of the parallel energy $(\langle\gamma_{\|}^2\rangle - \langle\gamma_{\|}\rangle^2)^{1/2}/\gamma_{\|0}$ as obtained from simulation (solid curve) and from theory (dashed curve) for the case without transverse focusing ($\gamma = 270$, $a_w = 2$, $\lambda_w = 5$ cm and $\langle\delta B_w^2\rangle^{1/2}/B_w = 0.3\%$).

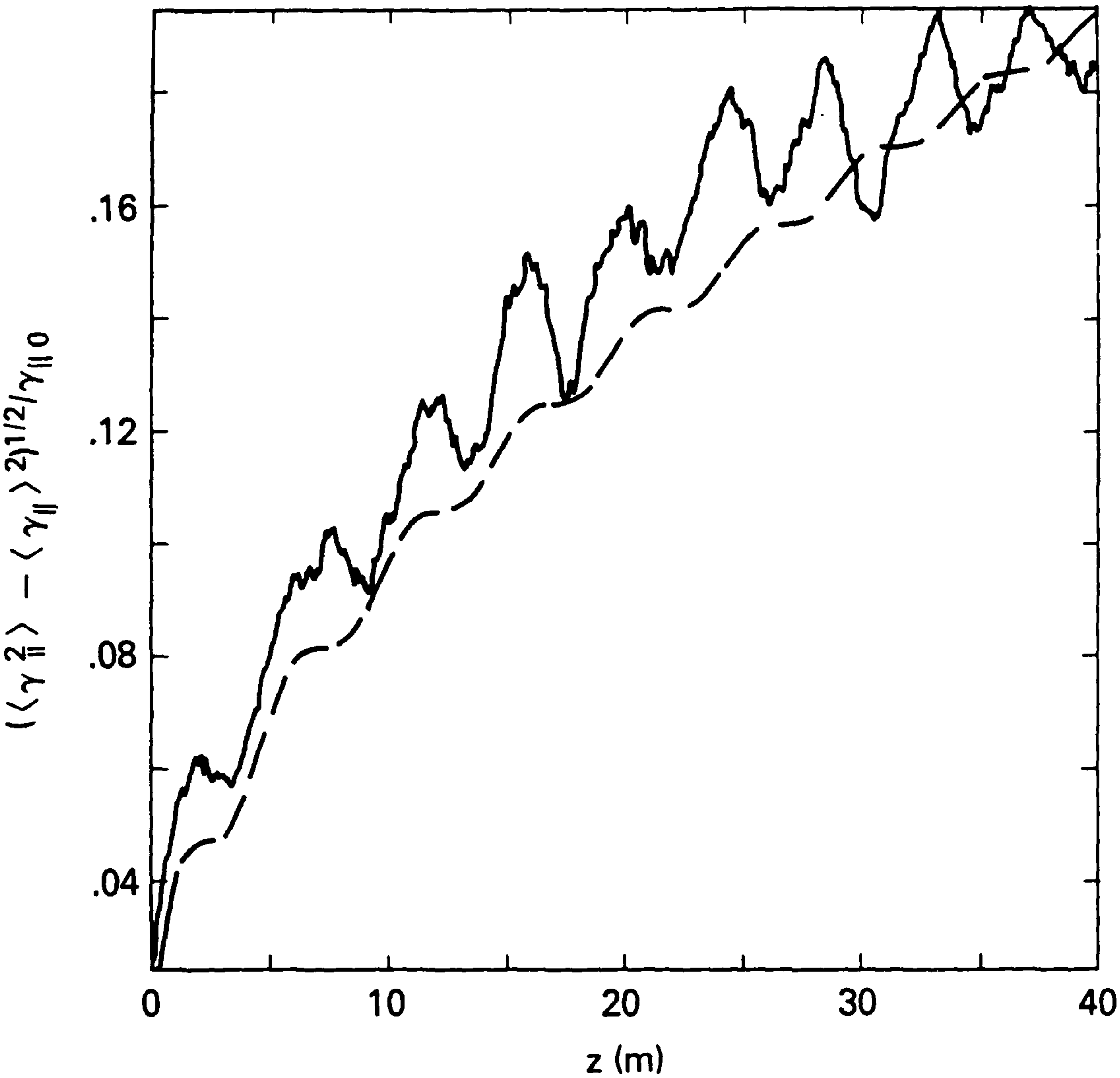

FIG. 12. The normalized variance of the parallel energy $(\langle\gamma_{\parallel}^2\rangle - \langle\gamma_{\parallel}\rangle^2)^{1/2}/\gamma_{\parallel 0}$ as obtained from simulation (solid curve) and from theory (dashed curve) for the case with transverse focusing ($\gamma = 270$, $a_w = 2$, $\lambda_w = 5$ cm and $\langle\delta B_w^2\rangle^{1/2}/B_w = 0.3\%$).

DISTRIBUTION LIST

Naval Research Laboratory
4555 Overlook Avenue, S.W.
Washington, DC 20375-5000

Attn: Code 1000 - Commanding Officer, CAPT J. J. Donegan, Jr.
1001 - Dr. T. Coffey
1005 - Head, Office of Management & Admin.
1005.1-Deputy Head, Office of Management & Admin.
1005.6-Head, Directives Staff
1200 - CAPT M. A. Howard
1201 - Deputy Head, Command Support Division
1220 - Mr. M. Ferguson
2000 - Director of Technical Services
2604 - NRL Historian
3000 - Director of Business Operations
4000 - Dr. W. R. Ellis
0124 - ONR
4600 - Dr. D. Nagel
4603 - Dr. W. W. Zachary
4700 - Dr. S. Ossakow (26 copies)
4700.1-Dr A. W. Ali
4790 - Dr. P. Sprangle
4710 - Dr. C. A. Kapetanakos
4710 - Dr. J. Mathew
4730 - Dr. R. Elton
4740 - Dr. W. M. Manheimer
4740 - Dr. W. Black
4740 - Dr. A. W. Fliflet
4740 - Dr. S. Gold
4740 - Dr. D. L. Hardesty
4740 - Dr. A. K. Kinkead
4740 - Dr. M. Rhinewine
4770 - Dr. G. Cooperstein
4790 - Dr. C. M. Tang (25 copies)
4790 - Dr. G. Joyce
4790 - Dr. M. Lampe
4790 - Dr. Y. Y. Lau
4790 - Dr. A. Ting
4790 - Dr. E. Esarey (25 copies)
4790 - Dr. J. Krall
4790A- B. Pitcher (25 copies)
5700 - Dr. L. A. Cosby
5745 - Dr. J. Condon
6840 - Dr. S. Y. Ahn
6840 - Dr. A. Ganguly
6840 - Dr. R. K. Parker
6843 - Dr. R. H. Jackson
6843 - Dr. N. R. Vanderplaats
6843 - Dr. C. M. Armstrong
6875 - Dr. R. Wagner
2628 - Documents (22 copies)
2634 - D. Wilbanks

Dr. R. E. Aamodt
Lodestar Research Corp.
2400 Central Ave., P-5
Boulder, CO 80306-4545

Dr. J. Adamski
Boeing Aerospace Company
P.O. Box 3999
Seattle, WA 98124

Dr. H. Agravante
TRW, Inc.
One Space Park
Redondo Beach, CA 90278 / R1-2020

Prof. I. Alexeff
University of Tennessee
Dept. of Electrical Engr.
Knoxville, TN 37916

Dr. L. Altgilbers
3805 Jamestown
Huntsville, AL 35810

Dr. A. Amir
Quantum Inst. and Dept. of Physics
University of California
Santa Barbara, CA 93106

Dr. Bruce Anderson
Lawrence Livermore National Laboratory
P. O. Box 808, L-436
Livermore, CA 94550

Dr. Antonio Anselmo
VARIAN
MS K-416
611 Hanson Way
Palo Alto, CA 94303

Dr. T. M. Antonsen
University of Maryland
College Park, MD 20742

Dr. Joseph Ashkenazy
M.I.T.
Research Lab. of Electronics
Room 36-219
Cambridge, MA 02139

Assistant Secretary of the
Air Force (RD&L)
Room 4E856, The Pentagon
Washington, D.C. 20330

Dr. W. P. Ballard
Sandia National Laboratories
ORG. 1231, P.O. Box 5800
Albuquerque, NM 87185

Dr. W. A. Barletta
Lawrence Livermore National Lab.
P. O. Box 808
Livermore, CA 94550

Dr. John J. Barnard
Lawrence Livermore Nat. Lab.
P. O. Box 808, L-626
Livermore, CA 94550

Dr. L. R. Barnett
3053 Merrill Eng. Bldg.
University of Utah
Salt Lake City, UT 84112

Project Manager
Ground Based Laser Project Office
ATTN: CSSD-H-F
White Sands Miss. Range, NM 88002-1198

CDR George Bates, PMS 405-300
Naval Sea Systems Command
Department of the Navy
Washington, DC 20362

Dr. W. Becker
Univ. of New Mexico
Institute for Mod. Opt.
Albuquerque, NM 87131

Dr. Robert Behringer
9342 Balcon Ave.
Northridge, CA 91325

Dr. G. Bekefi (5 copies)
Mass. Institute of Tech.
Room 36-213
Cambridge, MA 02139

Dr. S. Bender
Los Alamos National Laboratory
P. O. Box 1663
Los Alamos, NM 87545

Dr. J. Benford
Physics International
2700 Merced Street
San Leandro, CA 94577

Dr. Herbert S. Bennett
National Bureau of Standards
Bldg. 225, Rm. A352
Washington, DC 20234

Dr. Steven V. Benson
Physics Department
Stanford, CA 94305

Dr. I. B. Bernstein (10 copies)
Mason Laboratory
Yale University
400 Temple Street
New Haven, CT 06520

Dr. Vladislav Bevc
Synergy Research Institute
P.O. Box 561
San Ramon, CA 94583

Dr. Amitava Bhattacharjee
Columbia University
S. W. Mudd 210
Dept. of Applied Phys.
New York, NY 10027

Dr. Anup Bhowmik
Rockwell International/Rocketdyne Div.
6633 Canoga Avenue, FA-40
Canoga Park, CA 91304

Dr. K. Jim Bickford
RDA
2301F Yale Blvd., S.E.
Albuquerque, NM 87106

Dr. D. L. Birx
Lawrence Livermore National Laboratory
P. O. Box 808, L-627
Livermore, CA 94550

Dr. J. Bisognano
CEBAF
Newport News, VA 23606

Dr. Steve Bitterly
Rockwell International/Rocketdyne Div.
6633 Canoga Avenue, FA-40
Canoga Park, CA 91304

Dr. H. Boehmer
TRW DSSG
One Space Park
Redondo Beach, CA 90278

Dr. John Booske
Energy Research Bldg.
University of Maryland
College Park, MD 20742

Dr. P. Bosco
KMS Fusion Inc.
Ann Arbor, MI 48106

Dr. G. Bourianoff
1901 Rutland Drive
Austin, TX 78758

Dr. J. K. Boyd
Lawrence Livermore National Laboratory
P. O. Box 808
Livermore, CA 94550

Dr. E. Bozoki
NSLS
Brookhaven National Lab.
Upton, NY 11973

Dr. H. Brandt
Department of the Army
Harry Diamond Laboratory
2800 Powder Mill Rd.
Adelphi, MD 20783

Dr. R. Briggs
Lawrence Livermore National Lab.
MS-626
P.O. Box 808
Livermore, CA 94550

Dr. B. Hui
Defense Advanced Research Projects Agency
1400 Wilson Blvd.
Arlington, VA 22209

Dr. D. L. Bullock
Optical Sciences Department
TRW Space and Technology Group
Redondo Beach, CA 90278

Dr. Fred Burskirk
Physics Department
Naval Postgraduate School
Monterey, CA 93940

Dr. Ken Busby
Mission Research Corporation
1720 Randolph Road, S.E.
Albuquerque, NM 87106

Dr. K. J. Button
Francis Bitter Natl. Magnet Lab.
Box 72, M. I. T. Branch
Cambridge, MA 02139-0901

Dr. J. A. Byers
Lawrence Livermore National Lab.
Attn: (L-630)
P. O. Box 808
Livermore, CA 94550

Dr. Malcolm Caplan
4219 Garland Drive
Fremont, CA 94536

Dr. Maria Caponi
TRW, Building R-1, Room 1184
One Space Park
Redondo Beach, CA 90278

Dr. B. Carlsten
Los Alamos National Laboratory
MS-H827 AT-7
P. O. Box 1663
Los Alamos, NM 87545

Mr. A. Carmichael
GBL Project Office
ATTN: CSSD-H-F
White Sands Miss. Range, NM 88002-1198

Dr. David Cartwright
Los Alamos National Laboratory
E527
Los Alamos, NM 87545

Dr. J. Cary
University of Colorado
Box 391
Boulder, CO 80309

Prof. William Case
Dept. of Physics
Grinnell College
Grinnell, IA 50112

Mr. Charles Cason
U. S. Army Strategic Def. Command
ATTN: Code CSSD-H-D
P. O. Box 1500
Huntsville, AL 35807-3801

Dr. S. Caspi
Lawrence Berkeley Lab.
Bldg. 46
Berkeley, CA 94720

Dr. R. Center
Spectra Tech., Inc.
2755 Northup Way
Bellevue, WA 98004

Dr. K. C. Chan
Los Alamos National Laboratory
P. O. Box 1663
Los Alamos, NM 87545

Dr. V. S. Chan
GA Technologies
P.O. Box 85608
San Diego, CA 92138

Dr. Will E. Chandler
Pacific Missile Test Center
Code 3123
Point Muga, CA 93042-5000

Dr. J. Chase
Lawrence Livermore National Laboratory
P. O. Box 808
Livermore, CA 94550

Dr. S. Chattopadhyay
Lawrence Berkeley Laboratory
University of California, Berkeley
Berkeley, CA 94720

Prof. Frank Chen
School of Eng. & Applied Sciences
Univ. of Calif. at Los Angeles
7731 K Boelter Hall
Los Angeles, CA 90024

Dr. S. Chen
MIT Plasma Fusion Center
NW16-176
Cambridge, MA 01890

Dr. Yu-Juan Chen
L-626
Lawrence Livermore National Laboratory
P. O. Box 808
Livermore, CA 94550

Dr. D. P. Chernin
Science Applications Intl. Corp.
1720 Goodridge Drive
McLean, VA 22102

Dr. Art Chester
Hughes E51
Mail Stop A269
P.O. Box 902
El Segundo, CA 90245

Dr. S. C. Chiu
GA Technologies Inc.
P.O. Box 85608
San Diego, CA 92138

Dr. J. Christiansen
Hughes Aircraft Co.
Electron Dynamics Division
3100 West Lomita Blvd.
Torrance, CA 90509

Dr. T. L. Churchill
Spectra Technology, Inc.
2755 Northup Way
Bellevue, WA 98004

Major Bart Clare
USASDC
P. O. BOX 15280
Arlington, VA 22215-0500

Dr. Melville Clark
8 Richard Road
Wayland, MA 01778

Dr. Alan J. Cole
TRW
One Space Park
Redondo Beach, CA 90278

Dr. William Colson
Berkeley Research Assoc.
P. O. Box 241
Berkeley, CA 94701

Dr. Richard Cooper
Los Alamos National Scientific
Laboratory
P.O. Box 1663
Los Alamos, NM 87545

Dr. M. Cornacchia
Lawrence Berkeley Laboratory
University of California, Berkeley
Berkeley, CA 94720

Dr. R. A. Cover
Rockwell International/Rocketdyne Div.
6633 Canoga Avenue, FA-38
Canoga Park, CA 91304

Dr. D. Crandall
ER-55, GTN
Department of Energy
Washington, DC 20545

Mr. Thomas G. Crow
Ground Based Laser Project Office
ATTN: CSSD-H-FF
White Sands Missile Range, NM 88002-1198

Dr. Bruce Danly
MIT
NW16-174
Cambridge, MA 02139

Dr. R. Davidson (5 copies)
Plasma Fusion Center
Mass. Institute of Tech.
Cambridge, MA 02139

Dr. John Dawson (4 copies)
Physics Department
University of California
Los Angeles, CA 90024

Dr. David A. G. Deacon
Deacon Research
Suite 203
900 Welch Road
Palo Alto, CA 94304

Dr. Philip Debenham
Center for Radiation Research
National Bureau of Standards
Gaithersburg, MD 20899

Dr. T. L. Deloney
Dept. of Electrical Engineering
Stanford University
Stanford, CA 94305

Deputy Under Secretary of
Defense for R&AT
Room 3E114, The Pentagon
Washington, D.C. 20301

Prof. P. Diament
Dept. of Electrical Engineering
Columbia University
New York, NY 10027

Dr. N. Dionne
Raytheon Company
Microwave Power Tube Division
Foundry Avenue
Waltham, MA 02154

Director
National Security Agency
Fort Meade, MD 20755
ATTN: Dr. Richard Foss, A42
Dr. Thomas Handel, A243
Dr. Robert Madden, R/SA

Director of Research (2 copies)
U. S. Naval Academy
Annapolis, MD 21402

Dr. T. Doering
Boeing Aerospace Company
P.O. Box 3999
Seattle, WA 98124

Dr. Gunter Dohler
Northrop Corporation
Defense Systems Division
600 Hicks Road
Rolling Meadows, IL 60008

Dr. Franklin Dolezal
Hughes Research Laboratory
3011 Malibu Canyon Rd.
Malibu, CA 90265

Dr. A. Drobot
Science Applications Intl. Corp.
1710 Goodridge Road
McLean, VA 22102

Dr. Dwight Duston
SDIO/IST
The Pentagon
Washington, DC 20301-7100

Dr. Joseph Eberly
Physics Department
Univ. of Rochester
Rochester, NY 14627

Dr. Jim Eckstein
VARIAN
MS K-214
611 Hanson Way
Palo Alto, CA 94303

Dr. J. A. Edighoffer
TRW, Bldg. R-1
One Space Park
Redondo Beach, CA 90278

Dr. O. C. Eldridge
University of Wisconsin
1500 Johnson Drive
Madison, WI 53706

Dr. Luis R. Elias (2 copies)
Creol-FEL Research Pavillion
Suite 400
12424 Research Parkway
Orlando, FL 32826

Dr. C. James Elliott
X1-Division, M.S. 531
Los Alamos Natl. Scientific Lab.
P. O. Box 1663
Los Alamos, NM 87545

Dr. A. England
Oak Ridge National Laboratory
P.O. Box Y
Mail Stop 3
Building 9201-2
Oak Ridge, TN 37830

Dr. William M. Fairbank
Phys. Dept. & High Energy
Phys. Laboratory
Stanford University
Stanford, CA 94305

Dr. Anne-Marie Fauchet
Brookhaven National Laboratories
Associated Universities, Inc.
Upton, L.I., NY 11973

Dr. J. Feinstein
Dept. of Electrical Engineering
Stanford University
Stanford, CA 94305

Dr. Frank S. Felber
JAYCOR
11011 Torreyana Road
San Diego, CA 92121

Dr. D. Feldman
Los Alamos National Laboratory
P. O. Box 1663
Los Alamos, NM 87545

Dr. Renee B. Feldman
Los Alamos National Laboratory
P. O. Box 1663
Los Alamos, NM 87545

Dr. L. A. Ferrari
Queens College
Department of Physics
Flushing, NY 11367

Dr. C. Finfgeld
ER-542, GTN
Department of Energy
Washington, DC 20545

Dr. A. S. Fisher
Dept. of Electrical Engineering
Stanford University
Stanford, CA 94305

Dr. R. G. Fleig
Hughes Research Laboratory
3011 Malibu Canyon Road
Malibu, CA 90265

Dr. H. Fleischmann
Cornell University
Ithaca, NY 14850

Dr. E. Fontana
Dept. of Electrical Engineering
Stanford University
Stanford, CA 94305

Dr. Norwal Fortson
University of Washington
Department of Physics
Seattle, WA 98195

Dr. Roger A. Freedman
Quantum Institute
University of California
Santa Barbara, CA 93106

Dr. Lazar Friedland
Dept. of Eng. & Appl. Science
Yale University
New Haven, CT 06520

Dr. Walter Friez
Air Force Avionics Laboratory
AFWAL/AADM-1
Wright/Paterson AFB, OH 45433

Dr. Shing F. Fung
Code 696
GSFC
NASA
Greenbelt, MD 20771

Dr. R. Gajewski
Div. of Advanced Energy Projects
U. S. Dept of Energy
Washington, DC 20545

Dr. H. E. Gallagher
Hughes Research Laboratory
3011 Malibu Canyon Road
Malibu, CA 90265

Dr. James J. Gallagher
Georgia Tech. EES-EOD
Baker Building
Atlanta, GA 30332

Dr. W. J. Gallagher
Boeing Aerospace Co.
P. O. Box 3999
Seattle, WA 98124

Dr. J. Gallardo
Quantum Institute
University of California
Santa Barbara, CA 93106

Dr. E. P. Garate
15482 Pasedena Avenue, #120
Tustin, CA 92680

Dr. A. Garren
Lawrence Berkeley Laboratory
University of California, Berkeley
Berkeley, CA 94720

Dr. Richard L. Garwin
IBM, T. J. Watson Research Ctr.
P.O. Box 218
Yorktown Heights, NY 10598

Dr. J. Gea-Banacloche
Dept. of Physics & Astronomy
Univ. of New Mexico
800 Yale Blvd. NE
Albuquerque, NM 87131

DR. R. I. Gellert
Spectra Technology
2755 Northup Way
Bellevue, WA 98004

Dr. T. V. George
ER-531, GTN
Department of Energy
Washington, DC 20545

Dr. Edward T. Gerry, President
W. J. Schafer Associates, Inc.
1901 N. Fort Myer Drive
Arlington, VA 22209

Dr. Roy Glauber
Physics Department
Harvard University
Cambridge, MA 02138

Dr. B. B. Godfrey,
Chief Scientist
WL/CA
Kirtland AFB, NM 87117-6008

Dr. John C. Goldstein, X-1
Los Alamos Natl. Scientific Lab.
P.O. Box 1663
Los Alamos, NM 87545

Dr. Yee Fu Goul
Plasma Physics Lab., Rm 102
S.W. Mudd
Columbia University
New York, NY 10027

Dr. C. Grabbe
Department of Physics
University of Iowa
Iowa City, Iowa 52242

Dr. V. L. Granatstein
Dept. of Electrical Engineering
University of Maryland
College Park, MD 20742

Dr. D. D. Gregoire
Quantum Institute and Dept. of Physics
University of California
Santa Barbara, CA 93106

Dr. Y. Greenzweig
Quantum Inst. and Dept. of Physics
University of California
Santa Barbara, CA 93106

Dr. Morgan K. Grover
R&D Associates
P. O. Box 9695
4640 Admiralty Highway
Marina Del Rey, CA 90291

Dr. A. H. Guenther
Air Force Weapons Laboratory
Kirtland AFB, NM 87117

Lt Col Richard Gullickson
Strategic Def. Initiative Org.
OSD/SDIO/DEO
Washington, DC 20301-7100

Dr. K. Das Gupta
Physics Department
Texas Tech University
Lubbock, TX 79409

Dr. Benjamin Haberman
Associate Director, OSTP
Room 476, Old Exe. Office Bldg.
Washington, D.C. 20506

Dr. R. F. Hagland, Jr.
Director, Vanderbilt University
Nashville, TN 37235

Dr. K. Halbach
Lawrence Berkeley Laboratory
University of California, Berkeley
Berkeley, CA 94720

Dr. P. Hammerling
La Jolla Institute
P.O. Box 1434
La Jolla, CA 92038

Dr. John Hammond
Director, Directed Energy Office
SDIO
The Pentagon, T-DE Rm. 1E180
Washington, DC 20301-7100

Dr. R. Harvey
Hughes Research Laboratory
3011 Malibu Canyon Road
Malibu, CA 90265

Prof. Herman A Haus
Mass. Institute of Technology
Rm. 36-351
Cambridge, MA 02139

Dr. S. Hawkins
Lawrence Livermore National Laboratory
P. O. Box 808
Livermore, CA 94550

Dr. Carl Hess
MS B-118
VARIAN
611 Hanson Way
Palo Alto, CA 94303

Dr. K. Hizanidis
Physics Dept.
University of Maryland
College Park, MD 20742

Dr. A. H. Ho
Dept. of Electrical Engineering
Stanford University
Stanford, CA 94305

Dr. Darwin Ho
L-477
Lawrence Livermore National Laboratory
P. O. Box 808
Livermore, CA 94550

Dr. J. Hoffman
Sandia National Laboratories
ORG. 1231, P.O. Box 5800
Albuquerque, NM 87185

Dr. R. Hofland
Aerospace Corp.
P. O. Box 92957
Los Angeles, CA 90009

Dr. Fred Hopf
Optical Sciences Building, Room 602
University of Arizona
Tucson, AZ 85721

Dr. Heinrich Hora
Iowa Laser Facility
University of Iowa
Iowa City, Iowa

Dr. H. Hsuan
Princeton Plasma Physics Lab.
James Forrestal Campus
P.O. Box 451
Princeton, NJ 08544

Dr. James Hu
Quantum Inst. and Phys. Dept.
University of California
Santa Barbara, CA 93106

Dr. Benjamin Hubberman
Associate Director, OSTP
Rm. 476, Old Executive Office Bldg.
Washington, DC 20506

Dr. J. Hyman
Hughes Research Laboratory
3011 Malibu Canyon Road
Malibu, CA 90265

Dr. H. Ishizuka
University of California
Department of Physics
Irvine, CA 92717

Prof. V. Jaccarino
Univ. of Calif. at Santa Barbara
Santa Barbara, CA 93106

Dr. A. Jackson
Lawrence Berkeley Laboratory
University of California, Berkeley
Berkeley, CA 94720

Dr. S. F. Jacobs
Optical Sciences Center
University of Arizona
Tucson, AZ 85721

Dr. Pravin C. Jain
Asst. for Communications Tech.
Defense Communications Agency
Washington, DC 20305

Dr. E. T. Jaynes
Physics Department
Washington University
St. Louis, MO 63130

Dr. B. Carol Johnson
Ctr. for Radiation Research
National Bureau of Standards
Gaithersburg, MD 20899

Dr. Bernadette Johnson
Lincoln Laboratory
Lexington, MA 02173

Dr. G. L. Johnston
NW 16-232
Mass. Institute of Tech.
Cambridge, MA 02139

Dr. Shayne Johnston
Physics Department
Jackson State University
Jackson, MS 39217

Dr. R. A. Jong
Lawrence Livermore National Laboratory
P. O. Box 808/L626
Livermore, CA 94550

Dr. Howard Jory (3 copies)
Varian Associates, Bldg. 1
611 Hansen Way
Palo Alto, CA 94303

Dr. C. Joshi
University of California
Los Angeles, CA 90024

Dr. Paul Kennedy
Rockwell International/Rocketdyne Div.
6633 Canoga Avenue, FA-40
Canoga Park, CA 91304

Dr. R. Kennedy
Boeing Aerospace Company
P.O. Box 3999
Seattle, WA 98124

Dr. K. J. Kim, MS-101
Lawrence Berkeley Lab.
Rm. 223, B-80
Berkeley, CA 94720

Dr. I. Kimel
Creol-FEL Research Pavillion
Suite 400
12424 Research Parkway
Orlando, FL 32826

Dr. Brian Kincaid
Lawrence Berkeley Laboratory
University of California, Berkeley
Berkeley, CA 94720

Dr. A. Kolb
Maxwell Laboratories, Inc.
8835 Balboa Avenue
San Diego, CA 92123

Dr. Eugene Kopf
Principal Deputy Assistant
Secretary of the Air Force (RD&L)
Room 4E964, The Pentagon
Washington, D.C. 20330

Dr. P. Korn
Maxwell Laboratories, INc.
8835 Balboa Avenue
San Diego, CA 92123

Dr. S. Krinsky
Natl Synchrotron Light Source
Brookhaven National Laboratory
Upton, NY 11973

Prof. N. M. Kroll
Department of Physics
B-019, UCSD
La Jolla, CA 92093

Dr. Thomas Kwan
Los Alamos National Scientific
Laboratory, MS608
P. O. Box 1663
Los Alamos, NM 87545

Dr. Jean Labacqz
Stanford University
SLAC
Stanford, CA 94305

Dr. Ross H. Labbe
Rockwell International/Rocketdyne Div.
6633 Canoga Avenue, FA-40
Canoga Park, CA 91304

Dr. Willis Lamb
Optical Sciences Center
University of Arizona
Tucson, AZ 87521

Dr. H. Lancaster
Lawrence Berkeley Laboratory
University of California, Berkeley
Berkeley, CA 94720

Dr. D. J. Larson
Deptartment of Physics
University of Virginia
Charlottesville, VA 27901

Dr. J. LaSala
Physics Dept.
U. S. M. A.
West Point, NY 10996

Dr. Bernard Laskowski
M.S. 230-3
NASA-Ames
Moffett Field, CA 94305

Dr. Michael Lavan
U.S. Army Strategic Def. Command
ATTN: Code CSSD-H-D
P. O. Box 1500
Huntsville, AL 35807-3801

Dr. Ray Leadabrand
SRI International
333 Ravenswood Avenue
Menlo Park, CA 94025

Dr. Kotik K. Lee
Perkin-Elmer
Optical Group
100 Wooster Heights Road
Danbury, CT 06810

Dr. K. Lee
Los Alamos Nat. Scientific Lab.
Attn: X-1 MS-E531
P. O. Box 1663
Los Alamos, NM 87545

Dr. Barry Leven
NISC/Code 20
4301 Suitland Road
Washington, D.C. 20390

Dr. B. Levush
Dept. of Physics & Astronomy
University of Maryland
College Park, MD 20742

Dr. Lewis Licht
Department of Physics
Box 4348
U. of Illinois at Chicago Cir.
Chicago, IL 60680

Dr. M. A. Lieberman
Dept. EECS
Univ. of Cal. at Berkeley
Berkeley, CA 94720

Dr. Anthony T. Lin
Dept. of Physics
University of California
Los Angeles, CA 90024

Dr. Chuan S. Liu
Dept. of Physics & Astronomy
University of Maryland
College Park, MD 20742

Dr. D. D. Lowenthal
Spectra Technology
2755 Northup Way
Bellevue, WA 98004

Dr. A. Luccio
Brookhaven National Laboratory
Accelerator Dept.
Upton, NY 11973

Dr. A. Lumpkin
Los Alamos National Laboratory
P. O. Box 1663
Los Alamos, NM 87545

Dr. Phil Mace
W. J. Shafer Assoc., Inc.
1901 N. Fort Myer Drive
Arlington, VA 22209

Prof. J.M.J. Madey
117 Physics Bldg.
Duke University
Durham, NC 27706

Dr. R. Mako
205 South Whiting Street
Alexandria, VA 22304

Dr. Joseph Mangano
Science Research Laboratory
1600 Wilson Blvd.
Suite 1200
Arlington, VA 22209

Dr. Siva A. Mani
Science Applications Intl. Corp.
1040 Waltham Street
Lexington, MA 02173-8027

Dr. J. Mark
Lawrence Livermore National Lab.
Attn: L-477
P. O. Box 808
Livermore, CA 94550

Dr. T. C. Marshall
Applied Physics Department
Columbia University
New York, NY 10027

Dr. Xavier K. Maruyama
Dept. of Physics
Naval Postgraduate School
Monterey, CA 93943

Dr. Neville Marzwell
Jet Propulsion Lab.
MS 198-330
4800 Oak Grove Drive
Pasadena, CA 91109

Dr. A. Maschke
TRW
Mail Stop 01-1010
1 Space Park
Redondo Beach CA 90278

r. K. Matsuda
GA Technologies Inc.
P.O. Box 85608
San Diego, CA 92138

Dr. John McAdoo
8560 Cinderbed Road, Suite 700
Newington, VA 22122

Dr. D. B. McDermott
Electrical Engineering Dept.
University of California
Los Angeles, CA 90024

Dr. J. K. McIver
Dept. of Physics & Astronomy
Univ. of New Mexico
800 Yale Blvd. NE
Albuquerque, NM 87131

Dr. C. McKinstrie
Department of Mechanical Engineering
University of Rochester
Rochester, NY 14627

Dr. B. McVey
Los Alamos National Laboratory
P. O. Box 1663
Los Alamos, NM 87545

Dr. David Merritt
Space & Naval Warfare Command
Attn: PMW 145A
Washington, DC 20363-5100

Dr. John Meson
DARPA
1400 Wilson Boulevard
Arlington, VA 22209

Col Thomas Meyer
SDIO/DEO
The Pentagon, Rm. 1E180
Washington, DC 20301-7100

Dr. F. E. Mills
Fermilab
P.O., Box 500
Batavia, IL 60510

Dr. D. R. Mize
Hughes Research Laboratory
3011 Malibu Canyon Road
Malibu, CA 90265

Dr. Mel Month
Brookhaven National Laboratories
Associated Universities, Inc.
Upton, L.I., NY 11973

Dr. B. N. Moore
Austin Research Assoc.
1901 Rutland Dr.
Austin, TX 78758

Dr. Gerald T. Moore
University of New Mexico
Albuquerque, NM 87131

Dr. Warren Mori
1-130 Knudsen Hall
U.C.L.A.
Los Angeles, CA 90024

Dr. Philip Morton
Stanford Linear Accelerator Center
P.O. Box 4349
Stanford, CA 94305

Dr. Jesper Munch
TRW
One Space Park
Redondo Beach, CA 90278

Dr. James S. Murphy
National Synchrotron Light Source
Brookhaven National Laboratory
Upton, NY 11975

Prof. J. Nation
224 Phillips Hall
School of Elec. Eng.
Cornell University
Ithaca, NY 14850

Dr. R. Neighbours
Physics Department
Naval Postgraduate School
Monterey, CA 93943

Dr. George Neil
TRW
One Space Park
Redondo Beach, CA 90278

Dr. Kelvin Neil
Lawrence Livermore National Lab.
Code L-321, P.O. Box 808
Livermore, CA 94550

Dr. W. M. Nevins
L-639
Lawrence Livermore National Laboratory
P. O. Box 808
Livermore, CA 94550

Dr. Brian Newnam
MSJ 564
Los Alamos National Scientific Lab.
P.O. Box 1663
Los Alamos, NM 87545

Dr. W. Nexsen
Lawrence Livermore National Laboratory
P. O. Box 808
Livermore, CA 94550

Dr. Milton L. Noble (2 copies)
General Electric Company
G. E. Electric Park
Syracuse, NY 13201

Dr. K. O'Brien
Div. 1241 SNLA
Albuquerque, NM 87185

Dr. John D. O'Keefe
TRW
One Space Park
Redondo Beach, CA 90278

Dr. T. Orzechowski
L-436
Lawrence Livermore National Lab.
P. O. Box 808
Livermore, CA 94550

Prof. E. Ott (2 copies)
Department of Physics
University of Maryland
College Park, MD 20742

OUSDRE (R&AT)
Room 3D1067, The Pentagon
Washington, D.C. 20301

Dr. A. J. Palmer
Hughes Research Laboratory
3011 Malibu Canyon Road
Malibu, CA 90265

Dr. Robert B. Palmer
Brookhaven National Laboratories
Associated Universities, Inc.
Upton, L.I., NY 11973

Dr. J. Palmer
Hughes Research Laboratory
Malibu, CA 90265

Dr. Richard H. Pantell
Stanford University
Stanford, CA 94305

Dr. Dennis Papadopoulos
Astronomy Department
University of Maryland
College Park, Md. 20742

Dr. P. Parks
GA Technologies
P.O. Box 85608
San Diego, Ca 92138

Dr. John A. Pasour
Mission Research Laboratory
8560 Cinderbed Road
Suite 700
Newington, VA 22122

Dr. C. K. N. Patel
Bell Laboratories
Murray Hill, NJ 07974

Dr. Richard M. Patrick
AVCO Everett Research Lab., Inc.
2385 Revere Beach Parkway
Everett, MA 02149

Dr. Claudio Pellegrini
Brookhaven National Laboratory
Associated Universities, Inc.
Upton, L.I., NY 11973

Dr. S. Penner
Center for Radiation Research
National Bureau of Standards
Gaithersburg, MD 20899

Dr. J. M. Peterson
Lawrence Berkeley Laboratory
University of California, Berkeley
Berkeley, CA 94720

Dr. M. Piestrup
Adelphi Technology
13800 Skyline Blvd. No. 2
Woodside, CA 94062

Dr. Alan Pike
DARPA
1400 Wilson Boulevard
Arlington, VA 22209

Dr. Hersch Pilloff
Code 421
Office of Naval Research
Arlington, VA 22217

Dr. A. L. Pindroh
Spectra Technology
2755 Northup Way
Bellevue, WA 98004

Dr. D. J. Pistoresi
Boeing Aerospace Company
P. O. Box 3999
Seattle, WA 98124-2499

Major E. W. Pogue
SDIO
The Pentagon, T-DE Rm. 1E180
Washington, DC 20301-7100

Dr. Peter Politzer
General Atomic Tech., Rm. 13/260
P. O. Box 85608
San Diego, CA 92138

Major Donald Ponikvar
U. S. Army SDC
P. O. Box 15280
Arlington, VA 22245-0280

Dr. S. E. Poor
Lawrence Livermore National Laboratory
P. O. Box 808
Livermore, CA 94550

Prof. M. Porkolab
NW 36-213
Mass. Institute of Technology
Cambridge, MA 02139

Dr. R. V. Pound
Physics Department
Harvard University
Cambridge, MA 02138

Mr. J. E. Powell
Sandia National Laboratories
ORG. 1231, P.O. Box 5800
Albuquerque, NM 87185

Dr. Anand Prakash
Ballistic Research Laboratory
Aberdeen Proving Ground, MD 21005

Dr. Mark A. Prelas
Nuclear Engineering
Univ. of Missouri-Columbia
1033 Engineering
Columbia, Missouri 65211

Dr. Donald Prosnitz
Lawrence Livermore National Lab.
Box 5511 L-626
Livermore, CA 94550

Dr. D. C. Quimby
Spectra Technology
2755 Northup Way
Bellevue, WA 98004

Dr. Paul Rabinowitz
Xexon Research and Eng. Comp.
P. O. Box 45
Linden, NJ 07036

Dr. G. Ramian
Quantum Institute
University of California
Santa Barbara, CA 93106

Dr. L. L. Reginato
Lawrence Livermore National Laboratory
P. O. Box 808
Livermore, CA 94550

Dr. M. B. Reid
Dept. of Electrical Engineering
Stanford University
Stanford, CA 94305

Dr. D. A. Reilly
AVCO Everett Research Lab.
Everett, MA 02149

Dr. M. Reiser
University of Maryland
Department of Physics
College Park, MD 20742

Dr. S. Ride
Arms Control
Stanford University
Stanford, CA 94305

Dr. C. W. Roberson
Office of Naval Research
Code 112S
800 N. Quincy Street
Arlington, VA 22217

Dr. B. Robinson
Boeing Aerospace Company
P.O. Box 3999
Seattle, WA 98124

Dr. K. Robinson
Spectra Technology
2755 Northup Way
Bellevue, WA 98004

Dr. D. Rogers
Lawrence Livermore National Laboratory
P. O. Box 808
Livermore, CA 94550

Dr. Jake Romero
Boeing Aerospace Company
P. O. Box 3999
Seattle, WA 98124-2499

Dr. T. Romesser
TRW, Inc.
One Space Park
Redondo Beach, CA 90278

Dr. Marshall N. Rosenbluth
Dept. of Physics
B-019
Univ. of Calif., San Diego
LaJolla, CA 92093

Dr. J. B. Rosenzweig
The Inst. for Accelerator Physics
Department of Physics
University of Wisconsin-Madison
Madison, WI 53706

Dr. J. Ross
Spectra Technology
2755 Northup Way
Bellevue, WA 98004

Dr. N. Rostoker
Department of Physics
University of California at Irvine
Irvine, CA 92717

Dr. Antonio Sanchez
Lincoln Laboratory
Mass. Institute of Tech.
Room B213
P. O. Box 73
Lexington, MA 02173

Dr. Aldric Saucier
BMD-PO
Ballistic Missile Defense
Program Office
P. O. Box 15280
Arlington, VA 22215

Dr. A. Saxman
Los Alamos National Scientific Lab.
P. O. Box 1663, MSE523
Los Alamos, NM 87545

Dr. J. Scharer
ECE Dept.
Univ. of Wisconsin
Madison, WI 53706

Dr. E. T. Scharlemann
L626
Lawrence Livermore National Laboratory
P. O. Box 808
Livermore, CA 94550

Prof. S. P. Schlesinger
Dept. of Electrical Engineering
Columbia University
New York, NY 10027

Dr. Howard Schlossberg
AFOSR
Bolling AFB
Washington, D.C. 20332

Dr. George Schmidt
Stevens Institute of Technology
Physics Department
Hoboken, NJ 07030

Dr. M. J. Schmitt
Los Alamos National Laboratory
P. O. Box 1663
Los Alamos, NM 87545

Dr. Stanley Schneider
Rotodyne Corporation
26628 Fond Du Lac Road
Palos Verdes Peninsula, CA 90274

Dr. M. L. Scott
Los Alamos National Laboratory
P. O. Box 1663
Los Alamos, NM 87545

Dr. Richard L. Schriever (DP-23)
Director, Office of Inertial Fusion
U. S. Department of Energy
Washington, D.C. 20545

Dr. R. W. Schumacher
Hughes Research Laboratories
3011 Malibu Canyon Road
Malibu, CA 90265

Dr. H. Schwettmann
Phys. Dept. & High Energy
Physics Laboratory
Stanford University
Stanford, CA 94305

Dr. Marlan O. Scully
Dept. of Physics & Astronomy
Univ. of New Mexico
800 Yale Blvd. NE
Albuquerque, NM 87131

Dr. S. B. Segall
KMS Fusion
3941 Research Park Dr.
P.O. Box 1567
Ann Arbor, MI 48106

Dr. Robert Sepucha
DARPA
1400 Wilson Boulevard
Arlington, VA 22209

Prof. P. Serafim
Northeastern University
Boston, MA 02115

Dr. A. M. Sessler
Lawrence Berkeley Laboratory
University of California
1 Cyclotron Road
Berkeley, CA 94720

Dr. W. Sharp
L-626
Lawrence Livermore National Laboratory
P. O. Box 808
Livermore, CA 94550

Dr. Earl D. Shaw
Bell Laboratories
600 Mountain Avenue
Murray Hill, NJ 07974

Dr. J. P. Sheerim
KMS Fusion
P.O. Box 1567
Ann Arbor, MI 48106

Dr. R. Shefer
Science Research Laboratory
15 Ward Street
Somerville, MA 02143

Dr. R. L. Sheffield
Los Alamos National Laboratory
P.O. Box 1663
Los Alamos, NM 87545

Dr. Shemwall
Spectra Technology
2755 Northup Way
Bellevue, WA 98004

Dr. Shen Shey
DARPA/DEO
1400 Wilson Boulevard
Arlington, VA 22209

Dr. D. Shoffstall
Boeing Aerospace Company
P.O. Box 3999
Seattle, WA 98124

Dr. I. Shokair
SNLA, Org. 1271
Albuquerque, NM 87185

Dr. J. S. Silverstein
Harry Diamond Laboratories
2800 Powder Mill Road.
Adelphi, MD 20783

Dr. Jack Slater
Spectra Technology
2755 Northup Way
Bellevue, WA 98004

Dr. Kenneth Smith
Physical Dynamics, Inc.
P.O. Box 556
La Jolla, CA 92038

Dr. Lloyd Smith
Lawrence Berkeley Laboratory
University of California
1 Cyclotron Road
Berkeley, CA 94720

Dr. Stephen J. Smith
JILA
Boulder, CO 80302

Dr. Todd Smith
Hansen Labs
Stanford University
Stanford, CA 94305

Dr. J. Z. Soln (22300)
Harry Diamond Laboratories
2800 Powder Mill Road
Adelphi, MD 20783

Dr. G. Spalek
Los Alamos National Laboratory
P. O. Box 1663
Los Alamos, NM 87545

Mrs. Alma Spring
DARPA/Administration
1400 Wilson Boulevard
Arlington, VA 22209

SRI/MP Reports Area G037 (2 copies)
ATTN: D. Leitner
333 Ravenswood Avenue
Menlo Park, CA 94025

Dr. W. Stein
Los Alamos National Laboratory
P. O. Box 1663
Los Alamos, NM 87545

Dr. L. Steinhauer
STI
2755 Northup Way
Bellevue, WA 98004

Dr. Efrem J. Sternbach
Lawrence Berkeley Laboratory
University of California, Berkeley
Berkeley, CA 94720

Dr. W. C. Stwalley
Iowa Laser Facility
University of Iowa
Iowa City, Iowa 52242

Dr. R. Sudan
Lab. of Plasma Studies
Cornell University
Ithaca, NY 14850

Dr. P. V. Sumner
Hughes Research Laboratory
3011 Malibu Canyon Road
Malibu, CA 90265

Dr. David F. Sutter
ER 224, GTN
Department of Energy
Washington, D.C. 20545

Dr. Abraham Szoke
ML/L-470
Lawrence Livermore Natl. Lab.
P.O. Box 808
Livermore, CA 94550

Dr. T. Tajima
Institute for Fusion Studies
University of Texas at Austin
Austin, TX 78712

Dr. H. Takeda
Los Alamos National Laboratory
P. O. Box 1663
Los Alamos, NM 87545

Dr. J. J. Tancredi
Hughes Aircraft Co.
Electron Dynamics Division
3100 West Lomita Blvd.
Torrance, CA 90509

Dr. Milan Tekula
AVCO Everett Research Lab.
2385 Revere Beach Parkway
Everett, MA 02149

Dr. R. Temkin (2 copies)
Mass. Institute of Technology
Plasma Fusion Center
Cambridge, MA 02139

Dr. L. Thode
Los Alamos National Laboratory
P. O. Box 1663
Los Alamos, NM 87545

Dr. Keith Thomassen, L-637
Lawrence Livermore National Laboratory
P. O. Box 808
Livermore, CA 94550

Dr. Harold Thompson
TRW, Inc.
R1/2120
One Space Park
Redondo Beach, Ca 90278

Dr. Norman H. Tolk
Physics Department
Vanderbilt University
Nashville, TN 37240

Dr. Kang Tsang
Science Applications Intl. Corp.
1710 Goodridge Dr.
McLean, VA 22102

Dr. E. Tyson
Boeing Aerospace Company
P.O. Box 3999
Seattle, WA 98124

Dr. H. S. Uhm
Naval Surface Warfare Center
White Oak Lab.
Silver Spring, MD 20903-5000

Dr. L. Ulstrup
TRW, Inc.
One Space Park
Redondo Beach, Ca 90278

Under Secretary of Defense (R&D)
Office of the Secretary of Defense
Room 3E1006, The Pentagon
Washington, D.C. 20301

Dr. L. Vahala
Physics Dept.
College of William & Mary
Williamsburg, VA 23185

Dr. A. Valla
Spectra Technology
2755 Northup Way
Bellevue, WA 98004

Dr. A. Vetter
Boeing Aerospace Company
P.O. Box 3999
Seattle, WA 98124

Dr. A. A. Vetter
Spectra Technology
2755 Northup Way
Bellevue, WA 98004

Dr. G. Vignola
Brookhaven National Laboratories
Associated Universities, Inc.
Upton, L.I., NY 11973

Dr. S. A. Von Laven
KMS Fusion Inc.
Ann Arbor, MI 48106

Dr. John E. Walsh
Wilder Laboratory
Department of Physics (HB 6127)
Dartmouth College
Hanover NH 03755

Dr. Jiunn-Ming Wang
Brookhaven National Laboratories
Associated Universities, Inc.
Upton, L.I., NY 11973

Dr. T-S. Wang
Los Alamos National Laboratory
P. O. Box 1663
Los Alamos, NM 87545

Dr. J. F. Ward
Physics Department
1049 Randall
University of Michigan
Ann Arbor, MI 48109

Dr. Roger W. Warren
Los Alamos National Scientific Lab.
P.O. Box 1663
Los Alamos, NM 87545

Dr. J. Watson
Los Alamos National Laboratory
P. O. Box 1663
Los Alamos, NM 87545

Dr. B. Weber
Harry Diamond Laboratories
2800 Powder Mill Road
Adelphi, MD 20783

Dr. J. T. Weir
Lawrence Livermore National Laboratory
P. O. Box 808
Livermore, CA 94550

Ms. Bettie Wilcox
Lawrence Livermore National Lab.
ATTN: Tech. Info. Dept. L-3
P.O. Box 808
Livermore, CA 94550

Dr. Mark Wilson
National Bureau of Standards
Bldg. 245, Rm. B-119
Gaithersburg, MD 20899

Dr. H. Winick
Stanford Synch. Rad. Lab.
SLAC Bin 69
P.O. Box 44349
Stanford, CA 94550

Dr. J. Workman
Berkeley Research Associates
P.O. Box 241
Berkeley, CA 94701

Dr. Jack Wong (L-71)
Lawrence Livermore National Lab.
P. O. Box 808
Livermore, CA 94550

Dr. Thomas P. Wright
Sandia National Laboratories
ORG. 1231, P.O. Box 5800
Albuquerque, NM 87185

Dr. J. Wurtele
M.I.T.
NW 16-234
Plasma Fusion Center
Cambridge, MA 02139

Dr. Ming Xie
Dept. of Physics
Stanford University
Stanford, CA 94305

Dr. Edward Yadlowsky
High-Tech Research
P. O. Box 3422
Radford, VA 24143

Dr. Yi-Ton Yan
SSC Central Design Group
c/o LBL 90-4040
University of California
1 Cyclotron Road
Berkeley, CA 94720

Dr. A. Yariv
California Institute of Tech.
Pasadena, CA 91125

Dr. J. Yeh
Allied Corporation
31717 La Tienda Dr.
Westlake Village, CA 91362

Dr. A. Yeremian
Boeing Aerospace Company
P.O. Box 3999
Seattle, WA 98124

Dr. Barbara Yoou
R & D Associates
1401 Wilson Blvd., Suite 500
Arlington, VA 22209

Dr. Li Hua Yu
725B, NSLS
Brookhaven National Laboratory
Upton, NY 11973

Dr. Simon S. Yu
Lawrence Livermore National Laboratory
P. O. Box 808
Livermore, CA 94550

Dr. M. S. Zisman
Lawrence Berkeley Laboratory
University of California, Berkeley
Berkeley, CA 94720

Dr. J. Zumdieck
Spectra Technology
2755 Northup Way
Bellevue, WA 98004

Naval Research Laboratory
Washington, DC 20375-5000
Code 2630
Timothy Calderwood